Cement and Concrete Research 204 (2026) 108211

Contents lists available at ScienceDirect

Cement and Concrete Research

journal homepage: www.elsevier.com/locate/cemconres

Impact of the mineralogy of low–purity clays on their suitability as supplementary cementitious materials

Ilda Tole [a,*], Yuvaraj Dhandapani [b,c], Simon J. Kemp [d], Alastair T.M. Marsh [b], Clive Mitchell [d], Leon Black [b], Hong Wong [e], Susan A. Bernal [a,*]

[a] Department of Architecture and Civil Engineering, The University of Bath, Claverton Down, Bath, BA2 7AY, United Kingdom
[b] School of Civil Engineering, The University of Leeds, Woodhouse Ln, Leeds, LS2 9JT, United Kingdom
[c] Institute of Functional Surfaces, School of Mechanical Engineering, The University of Leeds, Woodhouse Ln, Leeds, LS2 9JT, United Kingdom
[d] British Geological Survey, Natural Environment Research Council, Environmental Science Centre, Keyworth, Nottingham, NG12 5GG, United Kingdom
[e] Centre for Infrastructure Materials, Department of Civil and Environmental Engineering, Imperial College London, South Kensington, London, SW7 2AZ, United Kingdom

ARTICLE INFO

Keywords:
Low–purity clays
Calcination
Supplementary cementitious materials
Mineralogy
Pozzolanicity
Characterisation

ABSTRACT

The lack of rapid screening and selection criteria limits the use of low–purity and common clays as supplementary cementitious materials (SCMs). Here the potential suitability as SCMs of 73 clays from 27 different geological formations, was investigated. Neither chemical composition nor kaolinite content were appropriate criteria to infer the calcined clays pozzolanic reactivity, which is the recommendation in existing guidelines. Clays exhibiting a total clay mineral content of ≥40 wt%, and a mica content below 60 wt% in the clay mineral fraction present moderate to high pozzolanic reactivity when calcined at 800 °C. Low–purity clays derived from kaolinitic Carboniferous formations, such as the Etruria and Pennine Coal Measures, consistently exhibited higher pozzolanic reactivity, compared with younger or marine–derived clays, particularly those from Jurassic, Cretaceous, and Quaternary aged-units. This new knowledge provides a novel guideline for the exploration and sourcing of promising clays for SCMs production globally.

1. Introduction

Reducing the embodied carbon of concrete production can be achieved by adopting several strategies, including reducing the clinker factor using cement replacements or supplementary cementitious materials (SCMs) in blended Portland cements [1–3]. However, an increase in global SCM production will be required to achieve the Global Cement and Concrete Association (GCCA) target of a 52% global average clinker factor in Portland cements by 2050 [4], from an estimated global average of 71% in 2018 [5]. Beyond reducing the CO_2 emissions, SCMs also enhance concrete durability and fosters industrial symbiosis within the supply chain. The latter is because the most widely used SCMs, such as fly ashes from coal combustion or blast furnace slags from iron making, are by–products from different industrial processes. However, the decarbonisation of these sectors will limit the availability of conventional SCM in some regions. Therefore, efforts are being made to identify locally available and abundant SCM sources to meet future demand [6]. Activated clays have been identified as effective and highly available SCMs, given the global abundance of natural clay resources in both top– and subsoils [2,7], or as waste streams from other activities (e.g. from mining operations, excavation works, among others) [8–10].

While limestone calcined clay cements (LC^3) [11,12] have demonstrated good mechanical properties [13] when produced using kaolinite-rich clays (typically containing ≥40 wt% kaolinite [14]), limited studies have been conducted on the effectiveness of other clay minerals such as montmorillonite [15,16], illite [17] or illite-chlorite [18]. Some research has shown the potential of producing effective SCMs from common clays, including low–purity clays with <40 wt% kaolinite [18–21], mixed illite–kaolinite clays [21–23], calcareous montmorillonite [24], or excavated and reclaimed clays [6,25–27]. However, uncertainties prevail, particularly when it comes to screening, selection and rapid estimation of their suitability as SCMs. This is mainly due to challenges associated with the accurate mineralogical characterisation of low–purity clays, compared to pure kaolinitic clays [7,28], and the limited understanding of how different clay properties, particularly mineralogical composition, influence their pozzolanicity once calcined.

* Corresponding authors.
E-mail addresses: it509@bath.ac.uk (I. Tole), sbl30@bath.ac.uk (S.A. Bernal).

https://doi.org/10.1016/j.cemconres.2026.108211
Received 31 October 2025; Received in revised form 17 February 2026; Accepted 15 March 2026
Available online 20 March 2026

Although they have been less studied, common and low–purity clays are promising feedstocks for SCM production due to their wide availability, established use in ceramics, and accessible sourcing from existing quarries and waste streams. The term 'common clays' generally refers to any naturally abundant clay deposit with mixed mineralogy that are used primarily for structural clay products, which are fine grained and typically exhibit plastic behaviour when wet [29]. In cement research, the term 'low–purity clays' is often used to describe clays with low amounts of reactive aluminosilicates, particularly those with low kaolinite content. Although not a formal geological classification, low–purity clays, like common clays, typically contain a mixture of clay minerals such as smectite, illite, chlorite, interstratified illite–smectite and kaolinite. These clay minerals form assemblages with non–clay minerals such as quartz, feldspar, mica, rutile, hematite, cristobalite, calcite, dolomite, pyrite etc., generating a complex mineralogical composition and, consequently, a wide range of properties and microstructure alterations induced by calcination of a given low–purity clay resource.

Upon calcination of kaolinite, dehydroxylation occurs and hydroxyl groups are released as water, resulting in the formation of metastable, anhydrous aluminium silicates like metakaolin, which exhibit high pozzolanic reactivity [9,30]. Conversely, non–kaolinitic clay minerals dehydroxylate over broader and often higher temperature ranges, and this process does not necessarily lead to complete amorphization [17,31]. Therefore, higher calcination temperatures are required to induce sufficient structural disruption to enhance their pozzolanicity [9,32]. In mixed–layer clays, dehydroxylation is influenced by the relative abundance of each mineral component and the overlapping thermal responses associated with their distinct characteristics [31,33]. For example, micas and chlorite typically undergo a two–step dehydroxylation process between 400–700 °C and 800–900 °C, reflecting the complexity of their layered structures [17,33,34]. Smectite dehydroxylates between 500 and 700 °C, depending on its chemical composition, impurities, and interlayer cations [33,35]. These mineralogical complexities often result in only partial dehydroxylation upon calcination, leading to a lower amorphous content and, consequently, reduced pozzolanic reactivity [16,36].

There are few studies (for example [20,22,32]) focusing on understanding how the mineralogical characteristics of non–kaolinitic clays (or 'low–purity clays') influence their chemical reactivity after calcination. Nevertheless, it has been observed that the kaolinite content seems to be the principal mineralogical factor determining reactivity after calcination for clays containing >40 wt% kaolinite [7]. For clays with low kaolinite contents, the reactivity of other clay minerals present becomes more significant [22]. For example, with an optimised calcination process illitic clays can develop a pozzolanic reactivity comparable to those of low– to medium–grade kaolinitic clays [18]. Furthermore, there is a limited understanding of how the geological provenance of common or low–purity clays influences their reactivity after calcination. For kaolinitic clays, it is known that highly weathered kaolinite tends to be more disordered and have a higher specific surface area; characteristics that lead to a faster dissolution kinetics after calcination [22,37]. But for low–purity clays, whilst the complexity and diversity of their mineralogy is well–known, the links between the geological formation, mineralogical characteristics and performance as an SCM are not yet established.

In low–purity clays, non–clay minerals such as quartz and hematite do not influence pozzolanicity, other than by dilution. Consequently, studies have centred on understanding the effect of carbonate minerals (inc. calcite, dolomite) commonly present in varying amounts. There is not yet a consensus on what upper limit of carbonate content is acceptable for a potential calcined clay, considering the trade–off between chemical reactivity and the potential offset of CO_2 savings, associated with their decomposition upon calcination. Clay reserves containing calcite or dolomite are used with caution due to the potential formation of reactive CaO and MgO during thermal activation. Contents of CaO and MgO are limited in current standards [39] to minimise the risk of durability issues; however, a CaO content in clays between 0.02 and 2.90 wt%, does not seem to negatively affect the pozzolanic activity [38]. Iron sulfides (e.g. pyrite) can also be present in low–purity clays, and are negatively perceived when present in calcined clays as they may induce severe cracking in concrete in alkaline media [40]. In the case of calcined clays, it has been reported that a calcination temperature as low as 650 °C is sufficient to fully oxidise pyrite, and its presence does not impact the chemical reactivity of the calcined clays [41].

Current standards include compositional requirements for calcined clays as SCMs, e.g. chemical oxide composition and loss on ignition value limits [42] with no mention of mineralogical composition, or minimum reactivity value. Reactivity testing is carried out through different methodologies including strength–based indices (e.g., Strength Activity Index in ASTM C618–23 [43]), chemical reactivity tests (e.g., Frattini test in EN 196–5 [44], reactive silica content in EN 196–2 [45], R^3 – ASTM C1897 [46]), or lime consumption methods (e.g., modified Chapelle test in NF P18–513 [47]). These methods reflect different underlying principles and are not directly equivalent, making it challenging to conduct a direct comparison of reactivity compliance across different standards. Also, low–purity clays are often not compliant with such requirements, as most standards were originally developed for calcined kaolinitic clays, blast furnace slag, and fly ashes. Consequently, there is an urgent need to develop robust screening and selection criteria to identify promising sources of low–purity clays to produce SCMs.

In response to the existing knowledge gaps associated with the selection of low–purity clays for producing SCMs, this study evaluated 73 low–purity clays across 27 different geological formations in the United Kingdom, sourced by the British Geological Survey (BGS). The clays were classified according to their mineralogical and lithostratigraphic characteristics, so that the results can assist the screening and selection of low-purity clays, with comparable mineral assemblages and geological provenance, from different regions globally. Based on analytical results (e.g. quantitative X-ray diffraction, thermogravimetry, surface area analysis), a classification system of four groupings is proposed. Twenty clays from across the four classification groups were then selected and calcined, and their chemical reactivity or pozzolanicity was measured according to the R^3 isothermal calorimetry method. Results were then analysed to determine the viability of using chemical or physical indicators as a proxy measure of mineralogical composition and pozzolanicity of low–purity clays. This approach establishes preliminary mineralogical selection guidelines for common or low–purity clays.

2. Experimental programme

2.1. Clays sourcing and pre–conditioning

In this study, in accordance with definitions provided in [25], the term "as–received clay" refers to the extracted material, prior to any pre–processing; "raw clay" to air–dried, crushed and homogenised; and "calcined clay" refers to the clay after being calcined in a laboratory furnace. Samples were labelled with the following coding approach: clays were numbered sequentially from 1 to 73, with the letter "C" preceding the number to identify the raw clay samples. When calcined, the clay name is preceded by an additional "C", for example, "C13" refers to raw clay sample number 13, and "CC13" refers to the corresponding calcined sample.

Sample sites were selected to provide both geological diversity and relevance to potential material use. They included primary sources (i.e. extraction from active quarry sites) as well as secondary sources (i.e. clay–bearing materials arising as by–products from industrial processes). Selection also reflected the availability of sites with ongoing extraction or industrial activity. The sampled geological formations included the Craven, Gala, Great Oolite, Kimmeridge, Lias, Lough Neagh, Mercia Mudstone, Millstone, Oxford Clay, Pennine Lower and Middle, and Wealden groups, as shown in Fig. 1. To ensure accurate

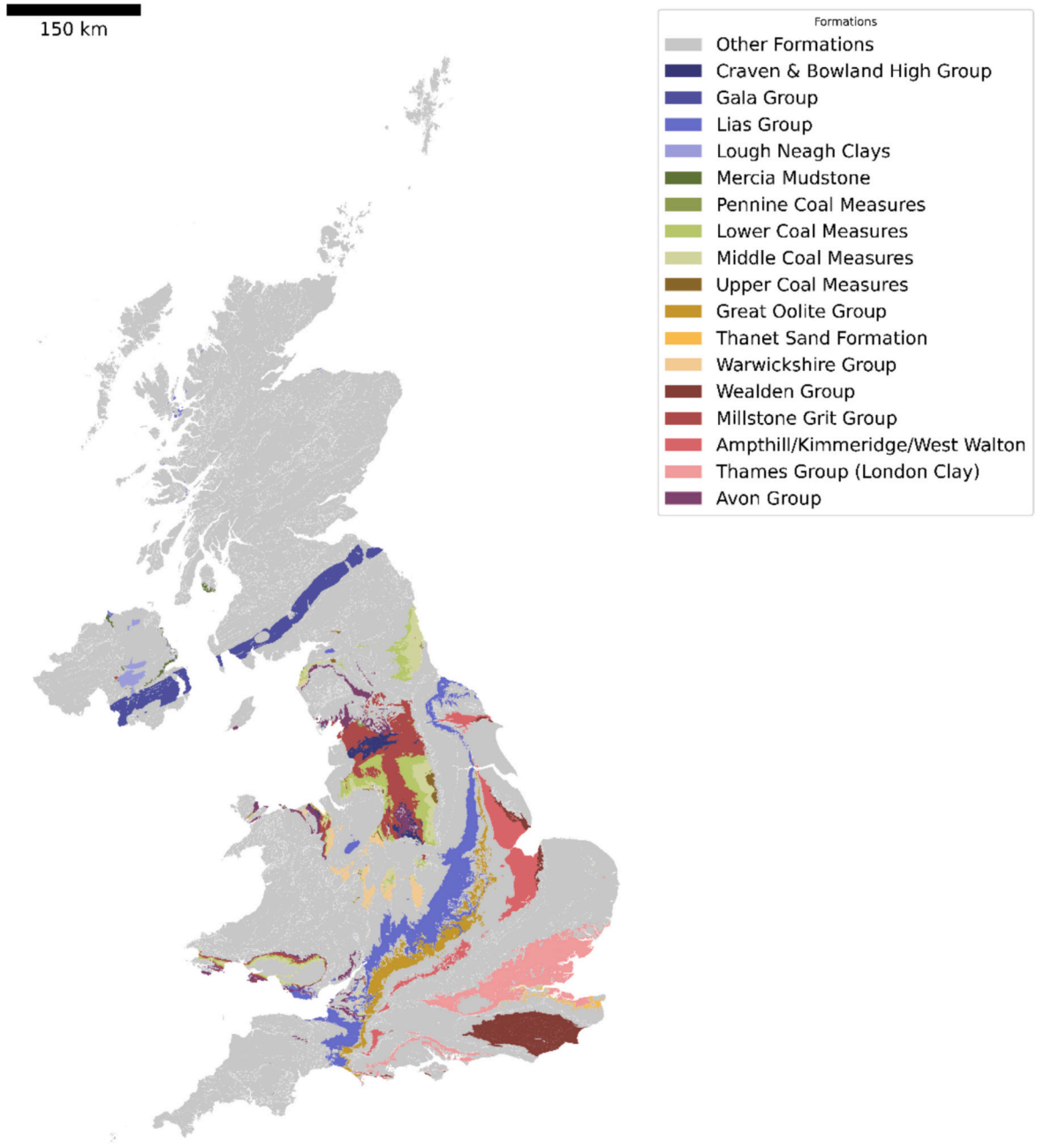

Fig. 1. Map illustrating the distribution of the UK geological locations where the clay samples were sourced. Map generated with the data from BGS.

representation of the characteristics of the clays, samples were homogenised from multiple points within each site.

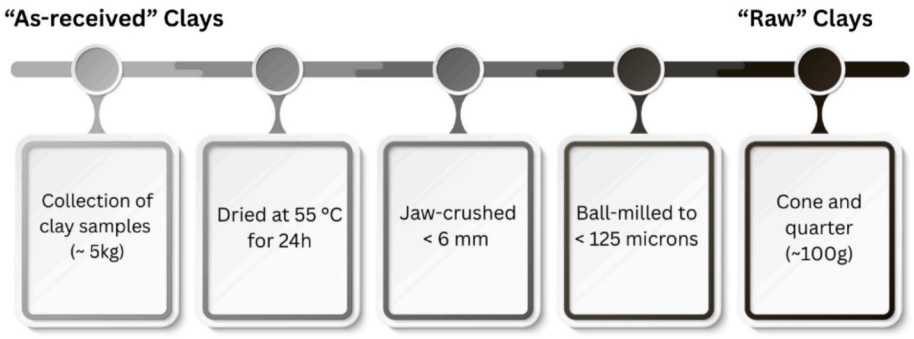

Fig. 2. Schematic of the process steps for the pre–conditioning of the as–received clays.

As illustrated in Fig. 2, each as–received clay sample (about 5 kg) was manually broken into small pieces and then placed in rectangular trays of 1 cm depth and in an oven at 55 °C for 24 h, to reach an air–dry state. The specimens were then crushed to <6 mm using a jaw crusher and subjected to ball milling to obtain a sample with particle size <125 μm for characterisation and calcination.

2.2. Characterisation of the raw clays

The specific surface area (SSA) of the raw clay samples was measured using the ethylene glycol monoethyl ether (EGME) method, described in [49], as previously applied to UK clay samples [50,51]. Approximately 1.1 g of each sample was dried under vacuum in a desiccator with anhydrous phosphorus pentoxide overnight. The samples were then saturated with 2–ethoxyethanol (EGME) and transferred to another desiccator containing calcium chloride. After 1.5 h, the desiccator was re–evacuated and left under vacuum overnight. The final weight was used to determine the amount of EGME absorbed, from which the surface area was calculated. A correction based on a pure smectite standard was then applied. SSA results are shown in **Table S1** in the Supplementary Information (SI) file.

The chemical composition of the raw clays was determined using X–ray fluorescence (XRF) spectroscopy, using a Rigaku ZSX Primus II, a fused bead preparation method, with the loss on ignition (LOI) determined after 1 h at 900 °C. The oxide compositions of the 73 raw clays evaluated are provided in the SI file, **Fig. S1**.

Mineralogical composition of the raw clays was determined by X-ray diffraction (XRD) (Malvern Panalytical X'Pert X-ray Diffractometer with Cobalt (CoKα, 1.79 Å source) on bulk powder and < 2 μm fractions to obtain bulk composition and the identification of clay mineral species, respectively. Quantitative XRD (QXRD) was conducted by Rietveld analysis using a 10% corundum (American Elements PN:AL–OX–03–P) internal standard using SiroQuant v5 software. Results are provided in the SI, Table S2.

Complementary thermogravimetric (TG) curves of the raw and calcined clays were obtained using a Netzsch STA 449 F5 attached to a mass spectrometer (Netzsch QMS 403D). Samples (~20 mg) were heated in alumina crucibles under flowing N_2 (60 mL/ min^1) using a programme started with a 30 °C isotherm for 10 min, followed by a 10 °C min^{-1} ramp up to 1000 °C. Mass spectrometry for mass/charge ratios of 18 and 44 were used to detect the released H_2O and CO_2 upon heating, respectively. The kaolinite content of the raw clays was quantified from the TG curves using the tangent method, where the dehydroxylation peak corresponding to kaolinite is delineated by tangents drawn to the onset and completion points of mass loss in the 400–650 °C range. Results for the mass loss curves are provided in the SI, **Fig. S2**.

2.3. Calcination procedure

Selected clays (selection criteria are discussed in 3.5) were calcined at 800 °C in porcelain dishes in batches of 300 g using a laboratory static furnace (Carbolite AAF 1100) with a dwell time at peak temperature of 1 h. This temperature was selected to screen the clays and enable consistent comparison across a diverse mineralogy, rather than to optimise activation for individual clay minerals. It is acknowledged that further optimisation of calcination temperature of the different clays, might be required. Nevertheless, the selected temperature allows for effective dehydroxylation of kaolinite without reaching temperatures where undesirable crystalline phases such as mullite and cristobalite form [52]. Although, 2:1 clay mineral such as illite and smectite require higher temperatures for dehydroxylation compared to 1:1 clay minerals such as kaolinite [8], 800 °C is considered a practical compromise, being sufficiently high to activate kaolinite and initiate the dehydroxylation of some 2:1 clay minerals while avoiding crystallisation [32]. Although slightly higher temperatures (850–900 °C) are often reported for industrial calcination, with varying residence times to ensure complete dehydroxylation of mineral phases, the selected temperature was adequate to calcine the samples evaluated.

2.4. Chemical reactivity of the calcined clays

The chemical reactivity or pozzolanic reactivity of the selected calcined clays was determined via the R^3 cumulative heat method (ASTM C1897–20) [53] and BS EN 196–12 (2024) [54] using a TAM Air isothermal calorimeter. Results were analysed to classify the calcined clays using reactivity thresholds established on 7–day cumulative heat values [55]. Selected calcined clays underwent additional R^3 testing for 14 days, to assess the potential chemical reactivity of low–purity clays that might not be captured within 7 days of testing.

3. Results and discussions

3.1. Specific surface area

The distribution of SSA for the raw clay samples is shown in Fig. 3, indicating substantial variability, with values ranging between 41 m^2/g to 307 m^2/g and a median value of 131 m^2/g. The SSA values reported here reflect the wide mineralogical variability of the clays assessed.

Several factors can influence the SSA of low–purity clays, including clay mineral type, diagenesis, and the presence of non–clay minerals. Clay minerals such as smectite make the greatest contribution to the internal surface area (i.e. area within their interlayer space between sheets) and external areas, whereas detrital minerals and carbonate minerals have a dilution effect on SSA [56]. The correlation between SSA and the mineralogical composition of the raw clays is discussed in **Section 3.8**.

From the practical perspective of producing SCMs, the particle size of the raw clay will have a significant impact on the chemical reactivity and performance of the calcined clay. Finer particles offer higher external surface area and therefore greater reactivity, while coarser particles limit the available surface for reaction. Considering that, non–kaolinitic clay minerals will need to be calcined at higher temperatures to induce structural alterations and enhance their pozzolanic reactivity [33,35]. The SSA and particle shape of the calcined clay will influence the workability [57] and hydration kinetics [57–60] of cementitious materials produced with them, so that finer particles will be more reactive, and rounded particles will likely enhance workability. Optimisation of the calcination process therefore needs to account for SSA variations of the raw clay, depending on the specific calcination

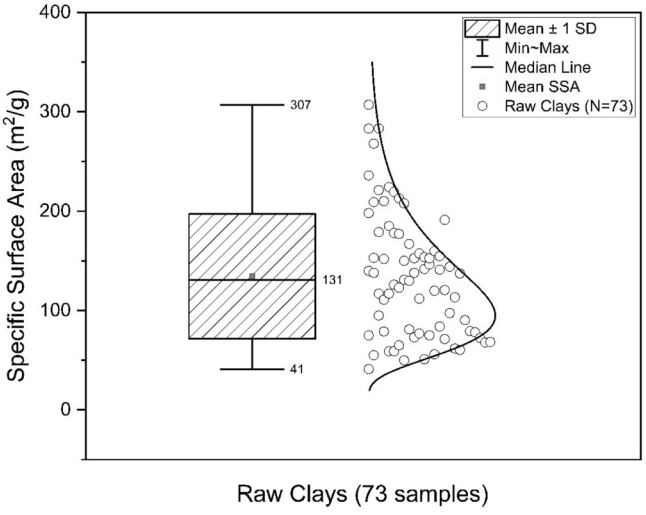

Fig. 3. Variation of the specific surface area (SSA) of the raw clay samples, measured by the EGME method.

process adopted (e.g. static furnaces, rotary kilns, or flash calcination), as the particle shape and particle size distribution for a given calcined clay would be different [59,61–63].

3.2. Chemical composition

The average values of the main oxides, as well as their minimum and maximum values across the analysed raw clay samples are summarised in Table 1.

In clays with a high clay mineral content or single-phase systems, kaolinite (and other 1:1 clay minerals) and 2:1 clay minerals can be distinguished by the higher Al_2O_3/SiO_2 ratio of kaolinite, reflecting its equal numbers of octahedral and tetrahedral sheets [64]. For relatively pure systems, higher Al_2O_3/SiO_2 ratios are commonly associated with increased kaolinite content. The Al_2O_3/SiO_2 ratios of the raw clays investigated in this study (Fig. 4) ranged from 0.10 to 0.52, with a mean value of 0.3, and one outlier at 0.90. However, the clays investigated here are low-purity materials, for which Al_2O_3/SiO_2 ratio is affected by other factors beyond the predominant clay mineral type, including the presence of siliceous minerals, the content of each clay mineral, and the extent of substitutions for Al and Si within the clay mineral structure. Consequently, the generally low Al_2O_3/SiO_2 ratios observed in this dataset reflect the compositional complexity of the clays rather than providing a reliable indicator of kaolinite content, consistent with the lack of correlation shown in Fig. 7.

The chemical composition of the raw clays in the $CaO–Al_2O_3–SiO_2$ system is shown in Fig. 5. The raw clays were higher in SiO_2 and lower in Al_2O_3 compared to pure 1:1 clays [65]. This indicates that the raw clays were mainly 2:1 type, or largely non–kaolinitic. Fig. 5 also shows that the oxide compositions of the clays were comparable with class F (low CaO) fly ashes for reference.

3.3. Compliance with existing standards

Calcined clays have been widely explored as SCMs, yet geographical differences exist. While standards in Asia, North America, and Europe are progressively evolving to accommodate a broader range of SCMs, significant gaps remain in addressing material performance and composition of the raw clay's specifications. In the European standard EN 197–1 [66], acceptance of pozzolans in blended cements is based on comparative mechanical performance, not accounting for the chemical or mineralogical characteristics of the raw clays, despite their critical influence on reactivity and long–term performance. The UK has two standards for natural and calcined natural pozzolans, with BS 8615–1 [67] covering natural pozzolana and their calcined forms, and BS 8615–2 [68] addressing high–reactivity calcined pozzolana. French, Indian, United States, and Chinese standards account for the chemical composition of the pozzolans, such as minimum contents of main oxides, limits on reactive CaO, MgO or SO_3, and/or loss on ignition (LOI). While maximum reactive CaO contents of 10 wt% and minimum main oxides contents of 70 wt% are generally accepted, MgO limits range from 3 to 5 wt%, and LOI limits vary between 4 and 10 wt%, as summarised in **Table S2** in SI file.

Table 1
Oxides composition of the raw clays evaluated.

Oxide	Raw clays (N = 73)		
	Minimum (wt%)	Mean (wt%)	Maximum
CaO	0.3	3.9	21.5
SiO_2	25.5	52.2	76.0
Al_2O_3	6.5	15.9	26.0
Fe_2O_3	3.8	7.0	24.7
Na_2O	0.1	0.6	1.8
K_2O	0.1	2.8	5.7
MgO	0.5	2.9	9.8
SO_3	0.03	0.5	3.9
TiO_2	0.3	0.9	3.0
LOI	1.1	12.2	35.6

The majority of the raw clays studied here comply with the compositional requirements specified in BS 8615–1 [67] for natural and natural calcined pozzolana. Fig. 6 illustrates the oxide composition threshold values for compliance. 53 clays presented a combined SiO_2, Al_2O_3, and Fe_2O_3 content ≥70 wt%. Only 17 of the 73 raw clays presented a CaO >10 wt%, after calcination. However, the results reported here include both reactive and non–reactive CaO forms, as it is not possible to distinguish the clear contribution of stable silicate minerals (e.g., plagioclase, which do not decompose at typical calcination temperatures) from XRF analysis alone. BS 8615–1 limits the maximum allowable SO_3 content to 3 wt%, and only two samples exceed this limit, suggesting that most of the raw clays evaluated would not pose a sulphate–related risk. SO_3 content is restricted in most SCM standards (**Table S2** in SI file) to prevent delayed ettringite formation and expansion [69], and interference with Portland cement setting time [70]. Overall, 46 of the 73 raw clays, met all four compositional requirements described above.

3.4. Mineralogical composition

The mineralogical composition of the raw clays, determined by QXRD analysis is shown in Table 2. The mineralogical composition is grouped into clay minerals, carbonates, silicates, and others.

Fig. 7 shows the results of Al_2O_3/SiO_2 ratio (Fig. 4) and kaolinite content (Table 2), where no direct relationship is observed. Therefore, chemical composition alone cannot be used as a proxy to infer kaolinite content in the low-purity clays evaluated.

The mineralogical compositions of the clays are illustrated in a ternary diagram (**Fig. 8**). The polar regions of the ternary diagram are used to categorise the clays as siliceous (rich in silica with main minerals including quartz, cristobalite, plagioclase, K–feldspar, pyroxene, zeolite), argillaceous (rich in clay minerals including micas, chlorite, kaolinite, smectite, mixed layered smectite/illite, palygorskite, corrensite), and calcareous (rich in calcium carbonates including calcite, aragonite, dolomite, Fe–dolomite, ankerite), with other minerals excluded from the plot.

In practice, this ternary diagram can assist raw material selection. For example, shale is argillaceous with smaller amounts of silica or carbonate, marl contains a mix of clay and carbonate, and siliceous mudstones are rich in quartz [71]. These lithologies (e.g. limestone, marl, and shale) are key feedstocks in Portland cement manufacturing. In this study, the same classification is adopted to explore the correlation between lithology and the roles of dominant mineral groups during calcination – knowing, for example, that siliceous minerals remain largely inert under thermal treatment; argillaceous minerals (e.g. kaolinite, smectites, and mixed–layer clays) represent the reactive clay fraction that transforms into amorphous pozzolanic phases upon dehydroxylation; and calcareous minerals decompose to release reactive CaO, which can either dilute or enhance reactivity depending on its interaction with aluminosilicates.

The examined raw clays predominantly fall into the argillaceous category (n = 40), with ten raw clays containing >75 wt% of clay minerals. A smaller proportion are siliceous clays (n = 17) and only one sample (C63) is classified as calcareous, indicating a composition primarily dominated by calcium carbonate.

The bulk mineralogical composition was analysed in relation to the type of clay minerals (Fig. 9). Kaolinite contents are relatively low (mean = 5 wt%, maximum ~55 wt%). Micaceous minerals, including illite and muscovite, were commonly present (median = 25 wt%), but exhibited the highest variability (0–58 wt%). The illite/smectite mixed-layer content ranged from 0 to 31 wt%, while chlorite was present in low amounts (≤20 wt%). Only a small proportion of the clays (n = 11) contained smectites. Total clay content showed significant variability, ranging from ~10 wt% to 88 wt% (Fig. 12B).

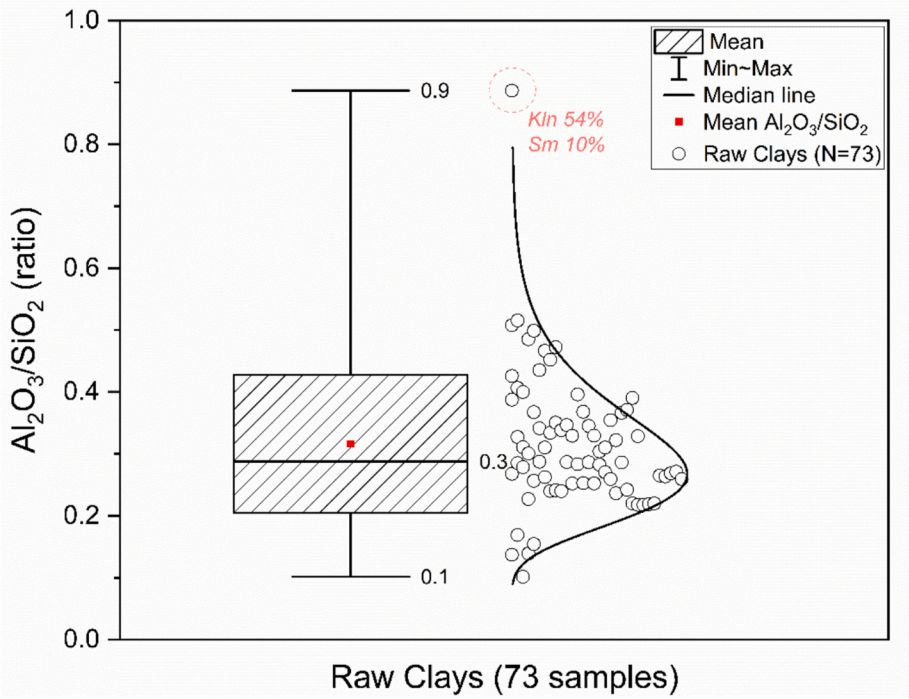

Fig. 4. Distribution of the Al_2O_3/SiO_2 ratio across all the 73 raw clays evaluated.

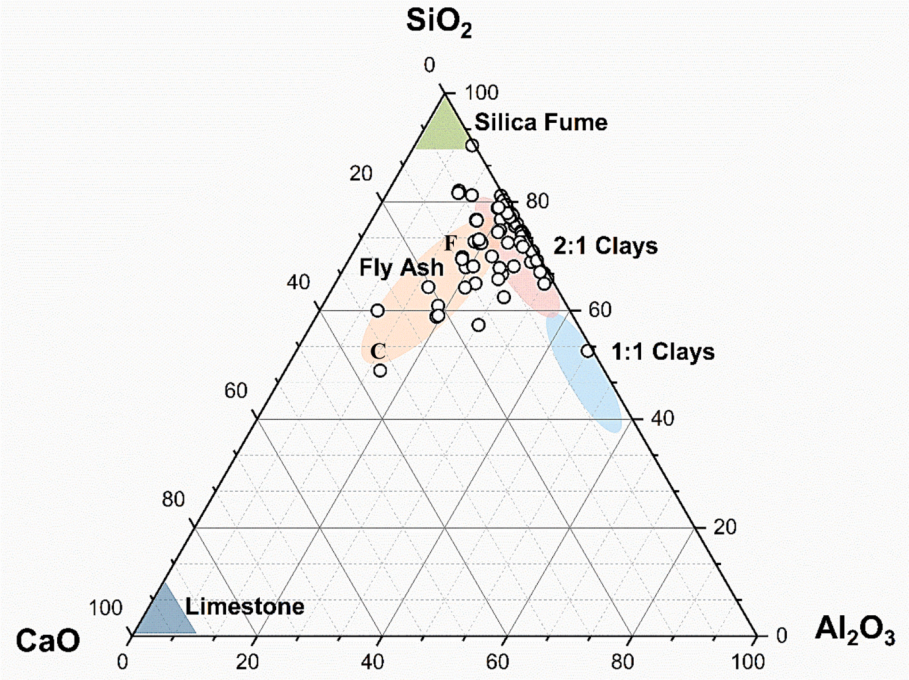

Fig. 5. Ternary diagram of the main oxides in the low–purity raw clays evaluated. The compositional regions of other SCMs and clay types in the diagram are adapted from [2,3].

Mineralogical analysis was also conducted on the <2 μm fractions (**Table S3** SI file) to definitively identify the clay minerals present (Fig. 10). In this fraction, the presence and distribution of micas and mixed–layers clays (e.g. corrensite and illite/smectite) were more easily discriminated than in the bulk of the raw clay, highlighting the micaceous nature of the studied clays.

3.5. Classification and grouping of the raw clays

Calcined clays derived from raw clays with moderate (40–60 wt%) [72] or low (15–40 wt%) kaolinite content can still perform effectively as SCMs [7,22]. Nevertheless, kaolinite content remains a key criterion for grouping the clays in this study, as it is the primary mineral phase known to govern reactivity upon calcination. Other criteria adopted for classifying the clays were the total carbonate and clay mineral content.

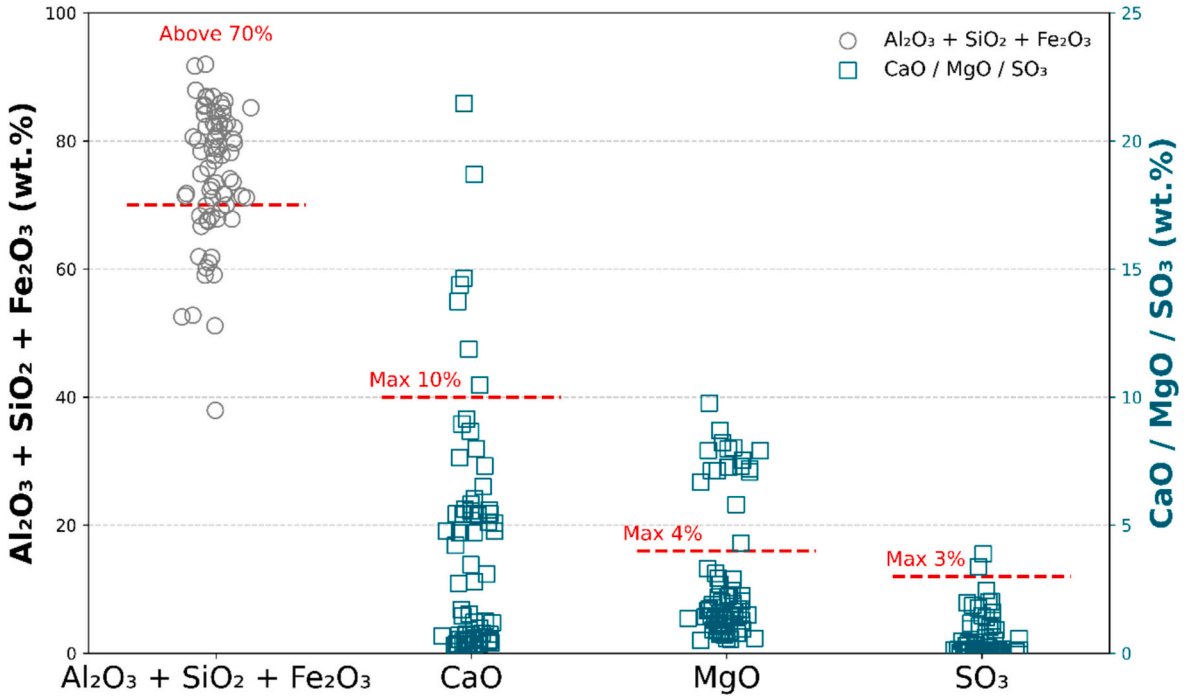

Fig. 6. Compliance with the standard requirement (BS 8615–1) of the raw clays ($N = 73$).

Table 2
Ranges of the minerals in the raw clay samples (N = 73) determined by QXRD.

Mineral	Minimum (wt%)	Average (wt%)	Maximum (wt%)
Clay minerals			
Mica	0.00	25.91	57.92
Chlorite	0.00	2.96	17.67
Kaolinite	0.00	12.70	54.76
Smectite	0.00	3.05	45.87
Illite/smectite	0.00	7.64	31.48
Palygorskite	0.00	0.01	0.50
Carbonates			
Calcite	0.00	5.15	38.91
Aragonite	0.00	0.21	6.12
Dolomite	0.00	3.45	35.26
Fe–Dolomite/ankerite	0.00	0.07	4.32
Siderite	0.00	0.58	10.96
Magnesite	0.00	0.04	2.10
Rhodocrosite	0.00	0.00	0.00
Silicates			
Quartz	0.40	28.08	73.02
Cristobalite	0.00	0.01	0.40
Plagioclase	0.00	3.39	35.86
K–feldspar	0.00	2.89	16.40
Pyroxene	0.00	1.34	40.10
Zeolite (chabazite)	0.00	0.85	44.10
Others			
Gypsum	0.00	0.33	5.90
Anhydrite	0.00	0.01	0.89
Jarosite	0.00	0.05	2.30
Anatase	0.00	0.06	1.01
Lepidocrocite	0.00	0.01	0.40
Hematite	0.00	0.62	4.45
Pyrite	0.00	0.43	6.00

The group classification developed in this study was established through a deductive reasoning process, based on known characteristics of constituent minerals and using this prior knowledge to define ranges of mineralogical composition. A similar classification approach, based on the mineralogical characteristics of clays, has previously been developed for the ceramics sector [73]. Although the clays evaluated present moderate to low kaolinite contents (see Table 2), this classification facilitates interpretation of the data. Considering kaolinite, total clay, and carbonate contents in the raw clays, four classification groups and their selection criteria are proposed (Fig. 11) and described below.

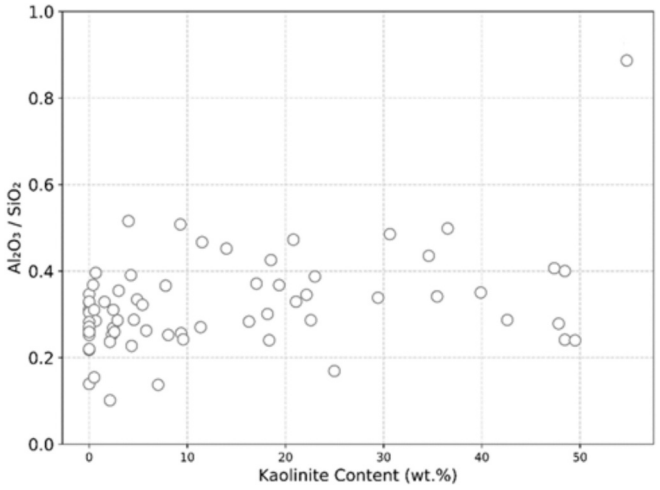

Fig. 7. Correlation between Al_2O_3/SiO_2 and kaolinite content of the 73 raw clays evaluated.

Group 1 clays contain kaolinite as the major clay mineral (> 40 wt %) (Fig. 12A), typically with micaceous minerals, and minor amounts of quartz or other impurities (< 5 wt%). Clays with similar mineralogical compositions have been extensively evaluated for the production of LC^3 type cements [74,75]. A total of 8 clays were identified in this group, with maximum kaolinite content of 54% and total clay content between 62 and 80 wt% (Fig. 12B).

Group 2 corresponds to clays with a high total clay mineral content (> 40 wt%) but lower kaolinite contents (15–40 wt%) (Fig. 12A), alongside smectites and small amounts of carbonates (<10 wt%). A total of 17 clays were identified that comply with these criteria.

Group 3 clays contain mixed clay mineral assemblages and high

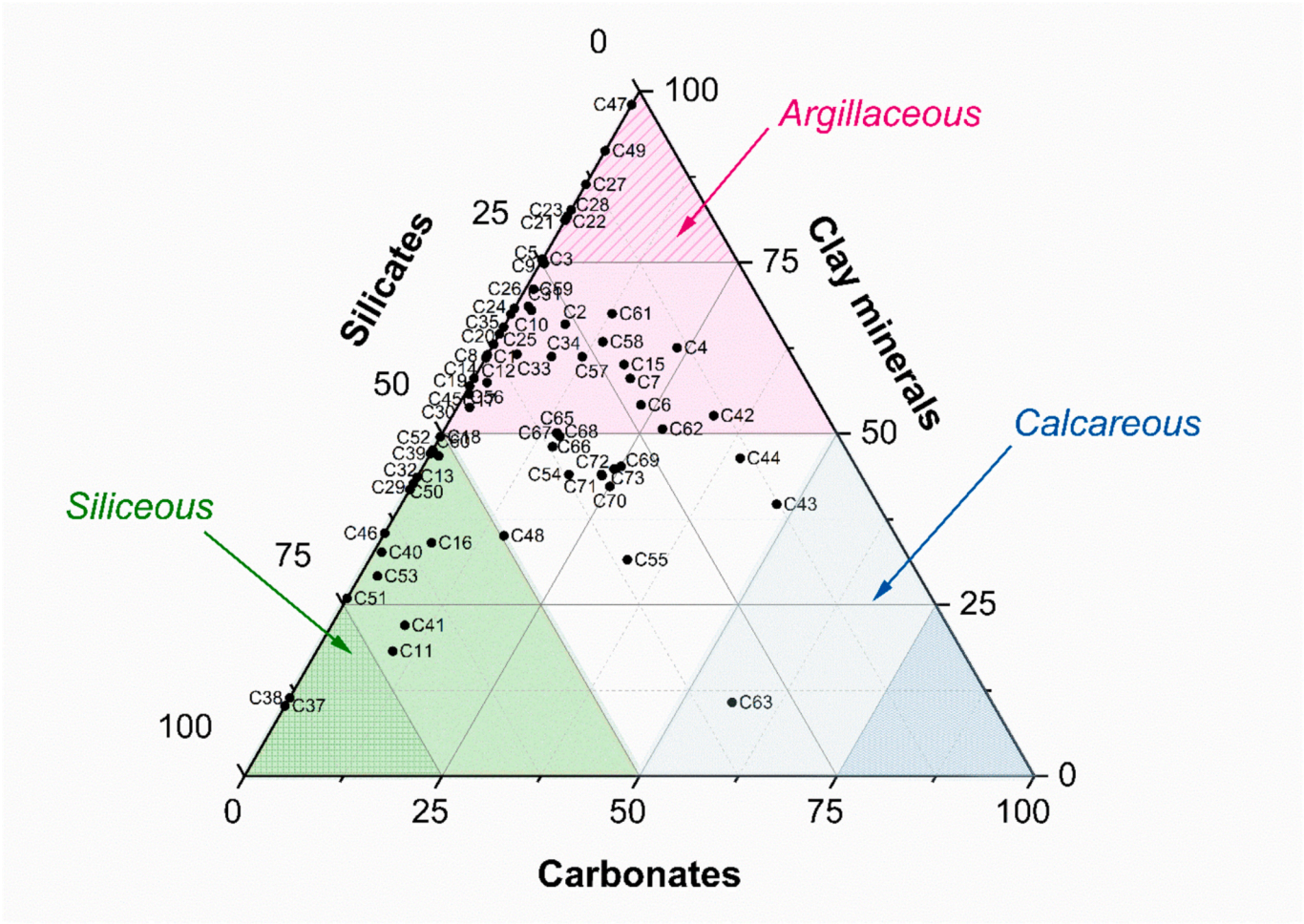

Fig. 8. Ternary diagram showing the mineralogical composition of the raw clays (n = 73) considering their content of clay minerals, carbonates, and silicates determined by QXRD.

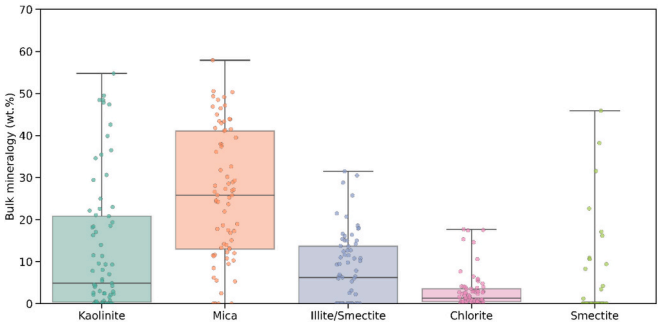

Fig. 9. Bulk mineralogy of the raw clays showing the content of the main clay minerals identified. The horizontal line within each box indicates the median value.

amounts (> 10 wt%) of carbonates (predominantly calcite or dolomite) (Fig. 12C). Previous studies have shown that calcite decomposes into free lime at calcination temperatures >820 °C, which can then react with metakaolin to form calcium aluminosilicate phases [76,77]. Although the effect of these reactions on reactivity is inconclusive (discussed in further detail in **Section 3.7**), the extra complexity of clays containing carbonates deserves distinct consideration. For this reason, these samples were classified separately to evaluate the specific effects of carbonate–rich low–purity clays on reactivity. In total, 27 clay samples were identified in this group.

Group 4 clays contain a mixture of clay minerals, with low kaolinite contents (<15 wt%) and higher micaceous mineral contents (mean = 50 wt%), Fig. 12B. Micaceous minerals are known to have relatively low chemical reactivity after calcination due to their resistance to structural breakdown. A total of 19 clays complied with these criteria.

Unclassified – Out of the 73 clays, three samples could not be classified into any of the proposed groups due to their distinctive compositions: two samples contained 75–85 wt% quartz, and one sample was composed of 40 wt% zeolites (e.g. chabazite) and 44 wt% pyroxene. Consequently, they were excluded from the following stages of the study.

In the following sections, results will be reported and analysed using these classifying groups to facilitate the identification of connections between the mineralogical composition of the clays evaluated and their performance as SCMs.

3.6. Thermogravimetric analysis

Thermogravimetric curves for all four groups are reported in the SI file, **Fig. S2.** The differential thermograms for the raw clays, grouped by mineralogical composition, are shown in Fig. 13. Results reveal three characteristic thermal events within each group: (I) dehydration between 50 and 300 °C, corresponding to the release of moisture and loosely bound water, (II) dehydroxylation of clay minerals between 350 and 950 °C, along with decomposition of minor organic matter and carbonates (calcite at 800–950 °C and dolomite at 600–950 °C [85]) and (III) recrystallisation at temperatures >950 °C [35,78].

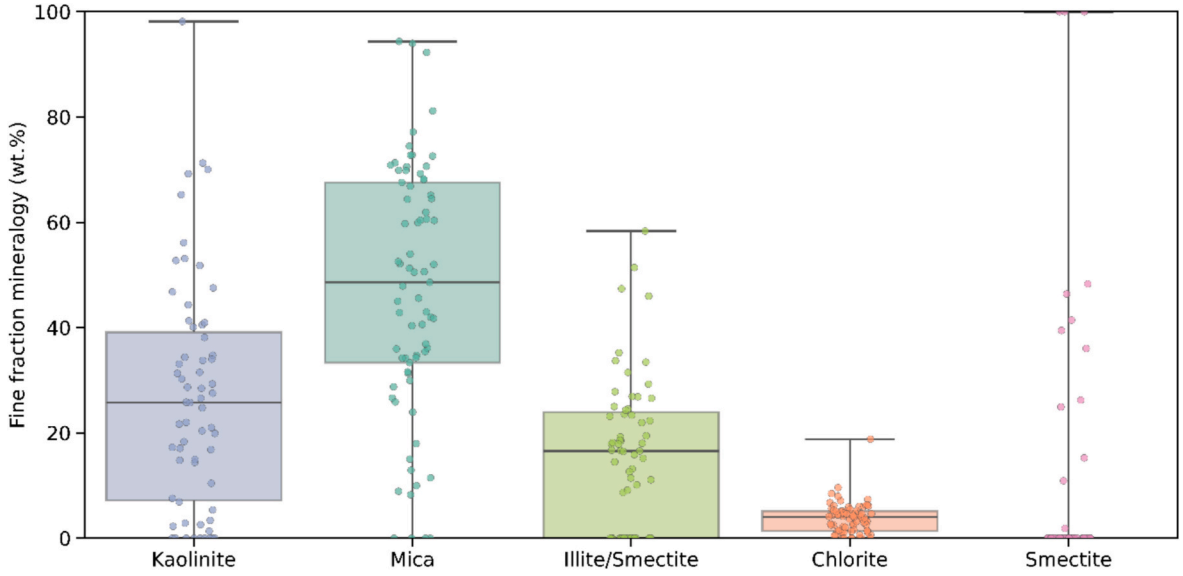

Fig. 10. Fine fraction mineralogy of raw clays, showing the content of clay minerals in the <2 μm fraction. The horizontal line within each box indicates the median value.

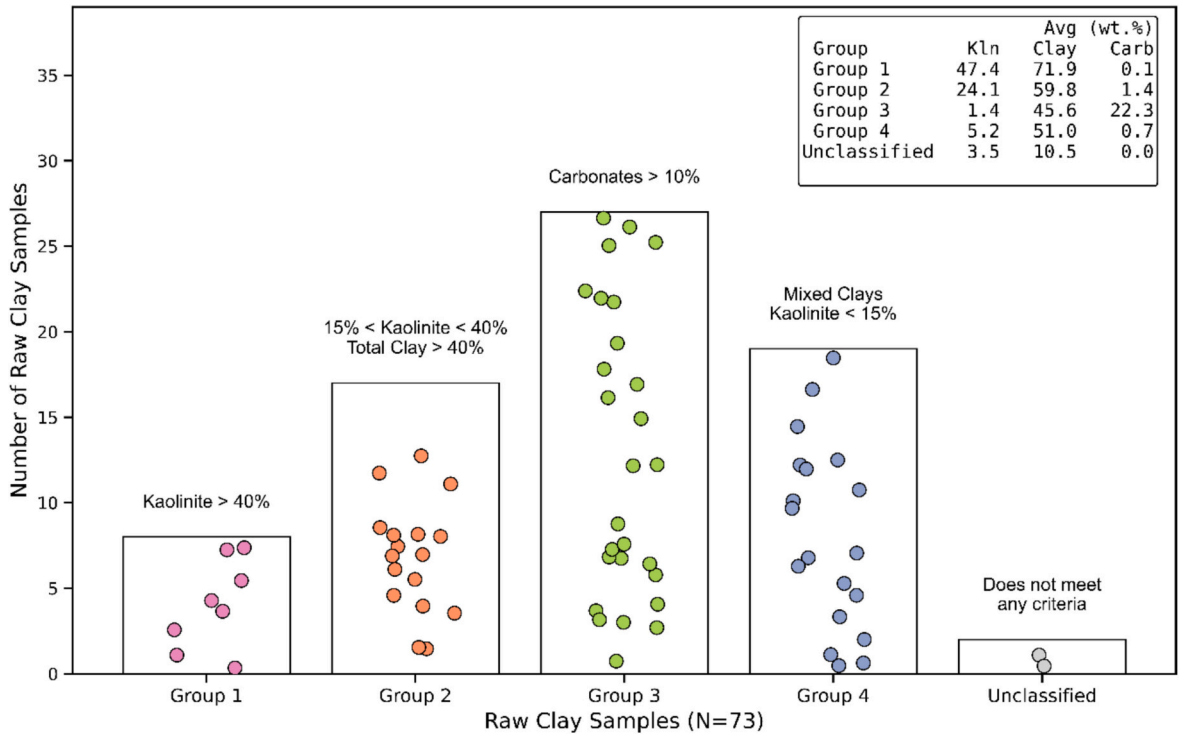

Fig. 11. Selection criteria and grouping of the raw clays based on kaolinite, total clay, and carbonate content. Dots within each bar represent individual raw clay samples, with vertical positions randomly assigned and not representing quantitative value. The inset table summarises the average kaolinite, total clay, and carbonate content for each group.

The temperature at which dehydroxylation occurs is strongly dependent on the clay mineral composition. Each clay mineral exhibits characteristic dehydroxylation behaviour during heating: kaolinite dehydroxylates in a single step typically between 420 and 600 °C [8]; the mica group (e.g., illite and muscovite) and chlorite undergo a two–step dehydroxylation at 400–700 °C and 800–900 °C [33,79]; and smectite generally dehydroxylates between 500 and 700 °C, with a peak at ~600–650 °C [80]. The dTG profile of a mixed–layer clay reflects the relative proportions and arrangement of the constituent minerals [31,33]. For example, in interstratified illite/smectite, dehydroxylation is often expressed as a single broad peak at an intermediate temperature, or occasionally as a double peak, indicating thermal contributions from both illitic and smectitic layers [33]. Due to this complexity, the mineralogical classification of the clays (in four groups) was used to support interpretation of their thermal behaviour, revealing consistent and characteristic dTG features within each classified group.

Group 1 clays exhibited a total mass loss at 1000 °C between ~8 to 12 wt% (Table 3). The curves from all clays in this group (Fig. 13A) showed a similar profile characterised by two main thermal events, the dehydration of free and adsorbed water (< 350 °C) and the

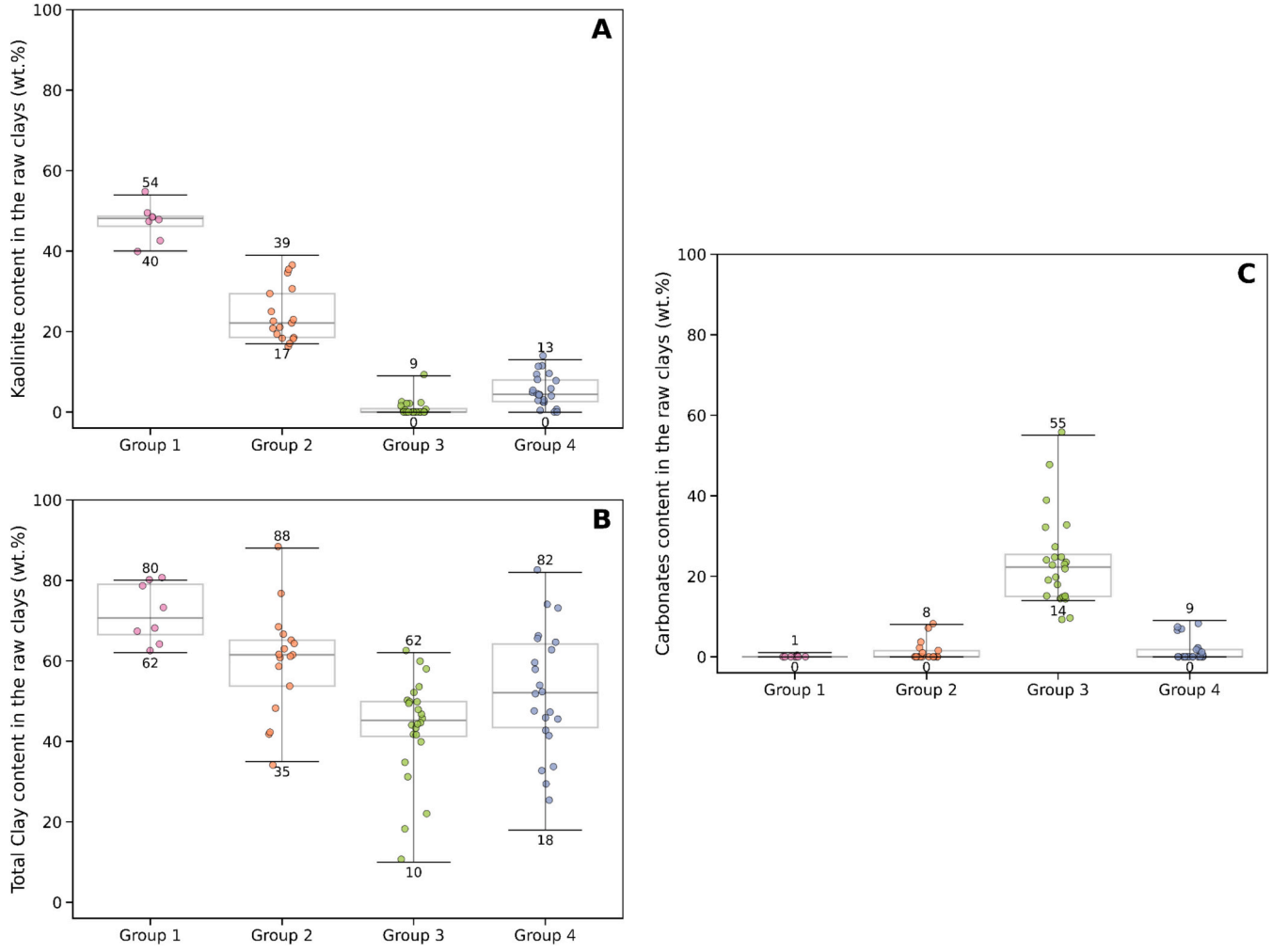

Fig. 12. Classification of the evaluated clays per group showing their distribution of **(A)** kaolinite content (wt%), **(B)** total clay content (wt%), and **(C)** total carbonates content (wt%) in the raw clays.

dehydroxylation of structural hydroxyls (400–650 °C). Samples C21, C22, and C23, with the highest kaolinite contents (47.4–49.5 wt%), exhibited the most pronounced dehydroxylation peak, within the typical kaolinite dehydroxylation range. Although primarily kaolinitic, these clays also contained other clay minerals such as micas and mixed layer illite/smectite. The latter undergoes dehydration over a broader temperature range (100–300 °C) than kaolinite, a behaviour that is also influenced by the presence of other phases (for example, sample C31 contained 3.5% gypsum, which may have contributed to this broader temperature range) [35]. Several raw clays (e.g., C25, C26) showed a distinct double peak around 250 °C (Fig. 13B), indicative of loss of interlayer water from clay minerals containing divalent interlayer cations [81].

Group 2 clays exhibited greater variability but showed a reduced mass loss to 1000 °C compared to Group 1, with values ranging from ~4 to 11 wt% (Table 3). Differential thermogravimetric analysis (Fig. 13B) revealed a mass loss below 200 °C, along with a smaller mass loss extending into the 200–300 °C range, associated with dehydration processes. Samples C10, C12, C14, C20, C27 (with kaolinite contents above 29 wt%) exhibited significant mass loss events in the 400–600 °C range, characteristic of kaolinite dehydroxylation. Additionally, several samples showed shoulders in the 600–800 °C region, associated with the dehydroxylation of other clay minerals such as illite and chlorite [8]. Mica–rich samples (e.g., C33, C34, C30 with >24 wt% of mica), also exhibited thermal events in this range, consistent with the two–step dehydroxylation behaviour typical of micas.

Group 3 clays, which contained >10 wt% carbonate minerals, exhibited increased mass loss to 1000 °C, ranging from ~8 to 20 wt%. The prominent mass loss occurring around 800 °C corresponds to the decomposition of these carbonate phases [81,83]. Compared to kaolinitic clays in Group 1 or mixed clays in Group 2, these samples exhibited limited mass loss around 500 °C, consistent with their low kaolinite contents (Fig. 13C) and minimal associated dehydroxylation in that temperature range. Most samples in Group 3, except for C41, contained high amounts of micaceous minerals (e.g., illite), which is evident from their thermal behaviour. Additionally, structural water loss in illite occurs over a broader temperature range and may produce multiple overlapping mass loss signals, as reflected in the gradual sloping curves observed across samples [82].

Group 4 clays exhibited a mass loss to 1000 °C of 5–15 wt% (Table 3), over a similar temperature range to Group 2 clays. These clays were primarily composed of micaceous, mixed–layer minerals and smectitic clays, with only minor amounts of kaolinite. Due to the high water adsorption capacity of smectites (e.g. montmorillonite), the mass loss peak with a maximum at ~150 °C, associated with the loss of adsorbed water, has a relatively large area [82]. Moreover, smectitic clays often exhibit double–shouldered peaks in the dehydration region, a feature present in several dTG profiles, indicating overlapping water release mechanisms. This interpretation is supported by the dTG curves, as several samples (e.g., C3, C5, C13) showed significant mass loss below 200 °C. Group 4 clays are characterised by impurities such as gypsum and zeolite, (SI, Table S2) which also contribute to mass loss below

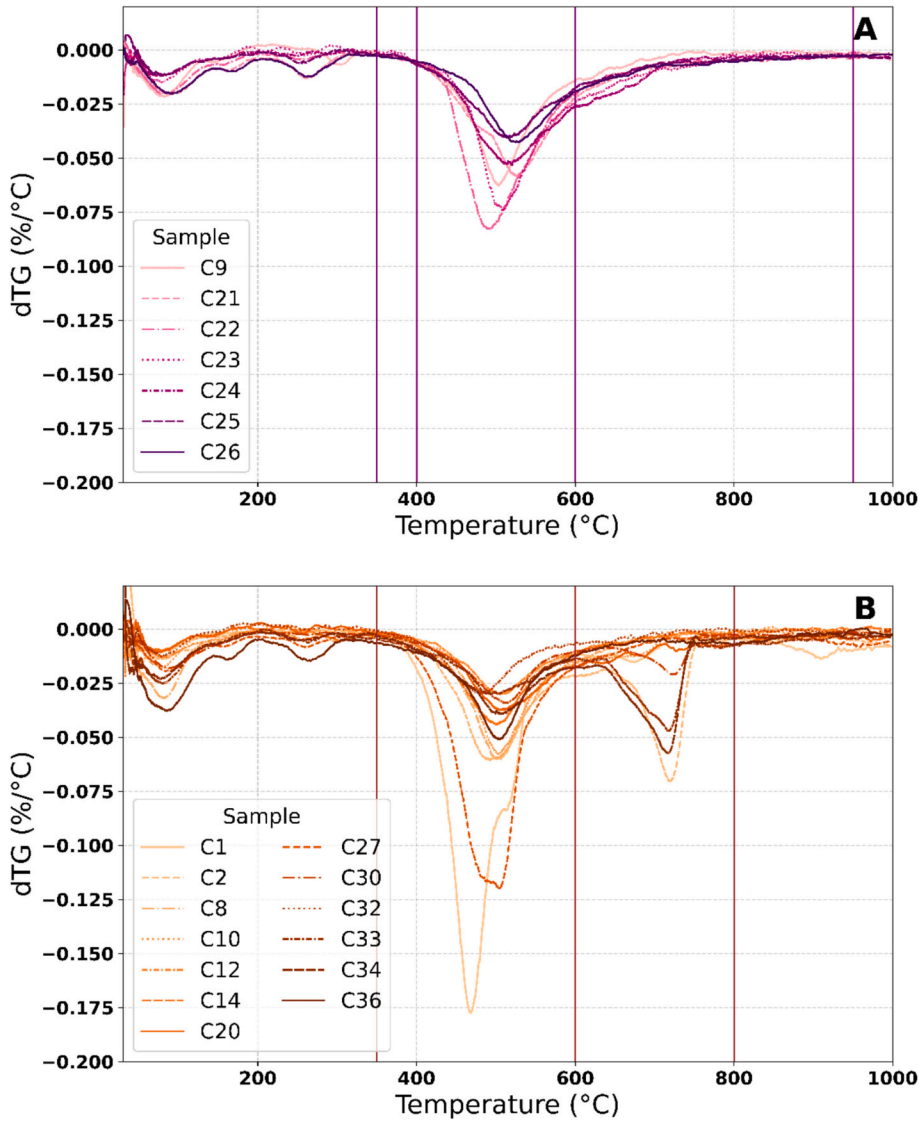

Fig. 13. Differential thermogravimetric analysis of the raw clays as function of the group classification, corresponding to **(A)** Group 1, **(B)** Group 2, **(C)** Group 3, and **(D)** Group 4.

200 °C [35].

Representative curves of mass loss, differential mass loss, H_2O (m/z = 18) and CO_2 (m/z = 44) released, for one selected clay from each mineralogical group, are presented in Fig. 14. Across all groups, mass loss at low temperatures (<200 °C) is associated with water release (Fig. 14A) as confirmed by the corresponding H_2O (m/z = 18) signals (Fig. 14C). The intensity of this peak reflects both physically adsorbed water and hydroxyl groups being expelled, which also aligns with the broader shoulders in the dTG curves. Group 1 (C21) and Group 2 (C32) showed a well–defined dehydroxylation peak around 500 °C (Fig. 14B and Fig. 14C). Sample C32 also exhibited CO_2 release over the same range (Fig. 14D), which may be attributed to the minor decomposition of organic matter or other volatile phases present in the clay [83]. Group 3 (C4) is particularly distinct due to a broad and pronounced release of CO_2 between 700 and 800 °C (Fig. 15D) consistent with carbonate mineral decomposition. XRD analysis identified calcite, dolomite and Fe–dolomite in this sample. The temperature range and intensity of CO_2 release indicate the presence of a significant quantity of carbonate minerals (e.g., calcite or dolomite [83]) undergoing thermal decomposition at elevated temperatures (C4 contains 23 wt% CaO). Moreover, Group 4 (C5) exhibits a broader and more gradual thermal profile and lower water release (Fig. 14C), suggesting less hydroxyl content or less reactive clays, consistent with their complex mineralogy (e.g., smectite and impurities).

To assess the consistency between analytical methods, kaolinite content determined by thermogravimetric analysis (TGA, using the tangent method) was compared to XRD bulk mineralogy. As shown in Fig. 15, the results revealed a systematic discrepancy between the two techniques. TGA yielded higher kaolinite values than XRD, particularly for samples in Groups 3 and 4, which had low kaolinite contents. The data suggest that TGA may overestimate kaolinite in low–purity clays, due to overlapping dehydroxylation signals from other clay minerals [28]. Since the estimation of kaolinite content can vary between different techniques, the use of kaolinite content alone as a sole indicator of clay composition, which is often linked to performance, e.g. chemical reactivity, compressive strength, among other [72] should be carefully interpreted, particularly for low–purity mixed clay sources. The two outliers reflect discrepancies between TGA and XRD quantifications arising from mineralogical interference. One sample shows TGA overestimation of kaolinite due to overlapping decomposition of other 2:1

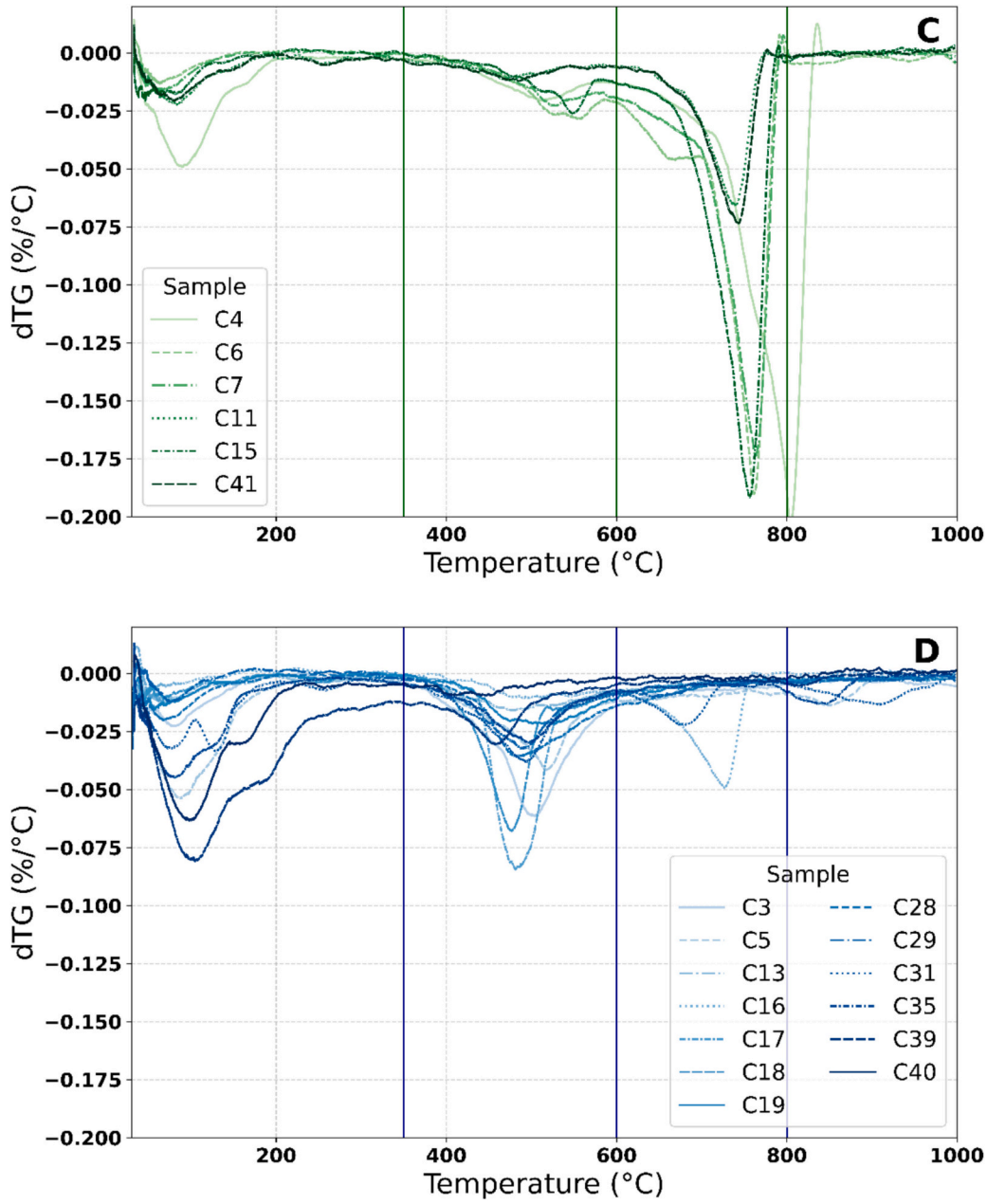

Fig. 13. (*continued*).

Table 3
Total mass loss of the raw clays evaluated via thermogravimetry analysis up to 1000 °C.

Clay group	Mass loss values (%)		
	Minimum	Mean	Maximum
1	7.9	10.0	12.2
2	4.5	8.2	11.3
3	7.8	13.9	20.3
4	4.9	8.4	14.6

clay minerals (~60 wt% of total clay content) and rhodochrosite (~13 wt%); similar effect for the other sample, where the underestimation may be linked to the high total clay content (~75 wt%).

3.7. Chemical reactivity of calcined clays

R^3 cumulative heat results for 1, 3, 7, and 14 days are reported in Fig. 16. Overall, most calcined clays (18 out of 20) exceeded the 7–day cumulative heat threshold for "moderate reactivity" [55] and can therefore be considered suitable SCMs. Also, calcination did not induce sufficient chemical reactivity in clays from Groups 3 and 4, consistent with their low kaolinite contents, high contents of micaceous minerals (which cannot be activated via calcination), and high carbonate contents.

To evaluate the influence of test duration on the R^3 isothermal calorimetry results, a linear regression analysis of cumulative heat release as a function of reaction time (Fig. 16) was conducted for the four clay groups. The observed changes in cumulative heat over time are statistically significant and not attributable to random variability, with probability of the observed change occurring by chance is being below 5% ($p < 0.05$). Comparing the cumulative heat between 7 and 14 days of

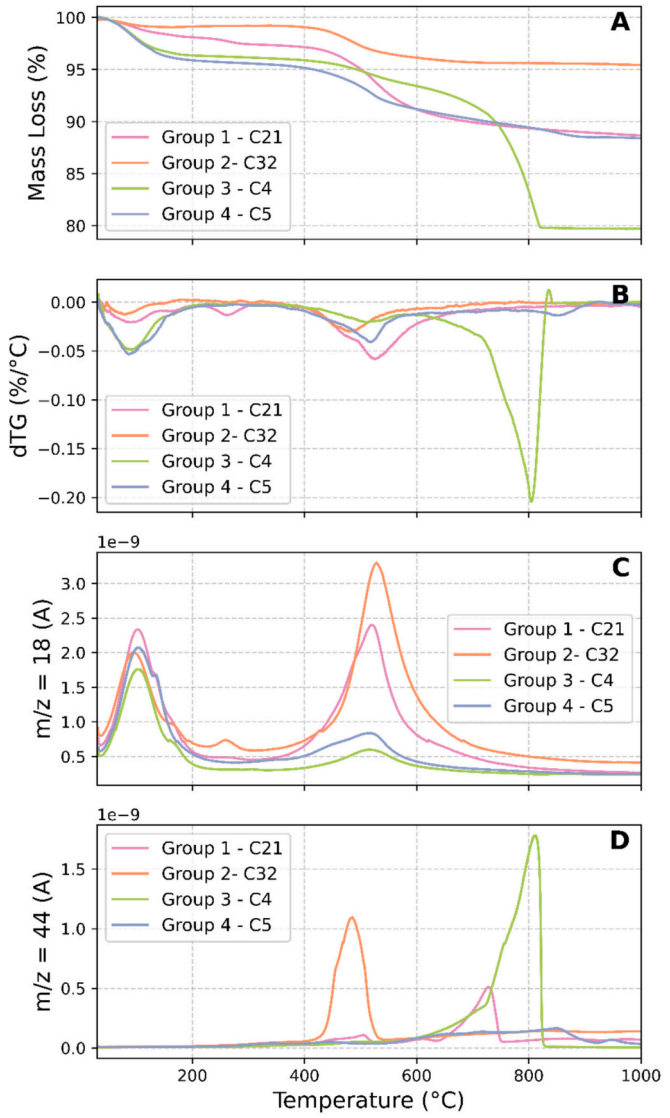

Fig. 14. **(A)** Thermogravimetric and **(B)** differential thermogravimetric curves of selected raw clays from each group, as well as mass spectrometry curves of **(C)** H_2O and **(D)** CO_2, as a function of the heating temperature.

testing (**Fig. S3** in SI file), there was a statistically significant increase for Groups 1 ($p = 0.023$), Group 2 ($p = 0.005$), 3 ($p = 0.004$), and 4 ($p = 0.016$) respectively.

Hence, R^3 isothermal calorimetry were examined up to 14 days for each selected clay within the group (Fig. 17), as sufficiently representative for the assessment of the pozzolanicity potential of low-purity clays.

Group 1 clays, with kaolinite content >40 wt%, exhibited the highest chemical reactivity at all the testing durations (Fig. 17A). Their cumulative heat release (384–570 J/g of SCM at 7 days; 433–693 J/g of SCM at 14 days, **Fig. S3** in SI file) falls within the moderately to highly reactive range, according to the classification in [55]. This is consistent with the R^3 results reported for calcined clays with >40% kaolinite content [84]. All samples showed continued heat evolution beyond 7 days, highlighting the importance of extended testing. Within this group, CC23 exhibited the highest cumulative heat (~693 J/g of SCMs at 14 days), consistent with its highest kaolinite content (49.5 wt%), presence of other clay minerals (16.8 wt% mica, 10.7 wt% illite/smectite, 3.5 wt% chlorite) and lowest quartz contents. CC9 also demonstrated high reactivity (~551 J/g of SCMs), although its kaolinite content (39.9 wt%) was slightly lower, likely due to mixed–layer clay's

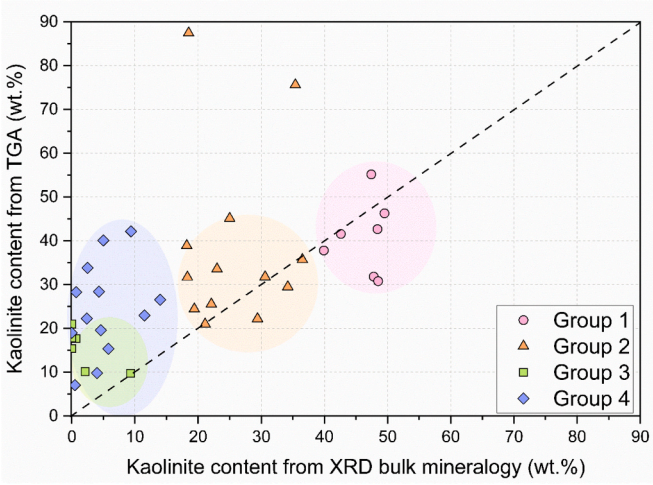

Fig. 15. Comparison between kaolinite content determined by TGA and XRD bulk mineralogy for four clay groups. The dashed line indicates the linear correlation.

contribution (illite/smectite at 30.5 wt%). Conversely, CC24 and CC26 showed lower reactivity (~454 and 433 J/g of SCMs respectively). Both had high kaolinite contents (>42 wt%) but also the highest quartz contents (26 wt%), which may have diluted the reactive mineral fraction. The reactivity ranking (CC23 > CC9 > CC24 ≈ CC26) is in good agreement with the combined influence of high kaolinite, low quartz, and the presence of other reactive clay mineral phases such as illite/smectite.

Group 2 clays contained 15–40 wt% kaolinite (Fig. 12A), often with illite/smectite, and showed a broad range of reactivities but consistently moderate range of reactivity. Cumulative heat release ranged from 218 to 413 J/g of SCMs at 7 days, and from 219 to 453 J/g of SCMs at 14 days. CC2 (453 J/g at 7 days), CC10 (425 J/g at 7 days), and CC36 (349 J/g at 7 days) exhibited the highest reactivity, whose values are comparable to those observed in some clays of Group 1. These clays all share low quartz contents and high total clay mineral contents (> 63 wt% total clay content, with kaolinite and mixed clays >45 wt%). Other Group 2 clays displayed lower reactivity. CC33, for example, showed the lowest heat release and remained near the reactivity threshold even after 14 days, consistent with its higher quartz and mica contents (25 wt% mica, 31 wt% quartz,13.7 wt% illite/smectite, and 22 wt% kaolinite). The analysis also suggested that high quartz content in some Group 2 clays (e.g. CC32 with 56.5 wt% quartz, and CC30 with 42.6 wt% quartz) might be the primary reason for their reduced performance. Well accepted guidelines specify that calcined clays used in LC^3 systems should be derived from raw clays containing at least 40% kaolinite as a mineralogical requirement for suitability as a source material [85].

Group 3 clays (Fig. 11) characterised by carbonate contents >10 wt % showed moderate reactivity overall. Their 7–day cumulative heat release ranged from 234 to 386 J/g of SCM, while 14–day values ranged from 294 to 421 J/g of SCM, indicating continued reactions between 7 and 14 days. The observed reactivity is mainly attributed to the relatively high total clay content (10–60 wt%), which likely contributed to the continued heat evolution, Fig. 12B. Although some clear trends are observed, further research is needed to better understand the mechanisms by which carbonate–rich clays affect reactivity and to optimise their use in blended cement systems. However, it is also important to note that the carbonate content may partially offset the intended CO_2 savings from using calcined clays. The decomposition of carbonate phases during calcination releases additional CO_2, and may also result in undesired performance effects, such as expansion, if significant amounts of free CaO or MgO are formed. Calcite or dolomite impurities may promote the formation of Ca-Si-Al-rich vitreous phases with low specific

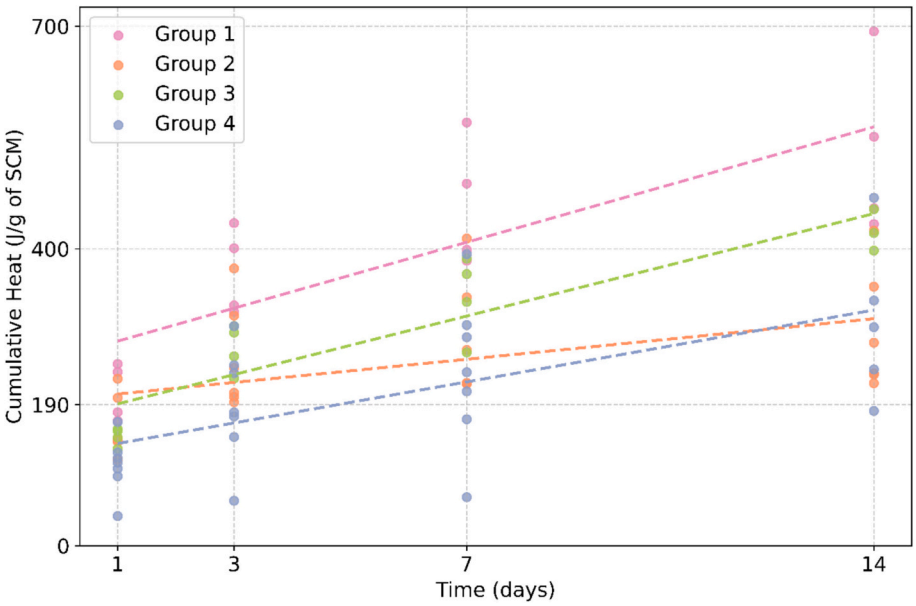

Fig. 16. Evolution of cumulative heat (J/g of SCM) with time for the four groups. Dashed lines represent linear regression of cumulative heat versus time. (Group 1: $R^2 = 0.6$; Group 2: $R^2 = 0.2$; Group 3: $R^2 = 0.8$; Group 4: $R^2 = 0.4$).

surfaces, which can limit their pozzolanic reactivity [77]. Blouch et al. [38] correlated calcined clay CaO content in LC^3 systems with compressive strength development, showing that higher CaO decreased 7–day compressive strength. However, this correlation was less pronounced at 28 days, suggesting that an excess of CaO may delay pozzolanic reactivity. Conversely, other studies [21,24,86,87] highlight the potential of using calcareous or carbonate–rich clays, indicating that, under optimised calcination conditions, they can form reactive calcium–aluminosilicate phases and perform effectively as SCMs.

Clays in **Group 4**, dominated by micaceous minerals and reduced kaolinite content, presented the lowest overall activity, ranging from 66 to 393 J/g after 7 days and from 180 to 469 after 14 days. Notably, some fell below the reactivity threshold, reflecting the lower reactivity of micaceous phases. CC28 (58 wt% mica and 16 wt% illite/smectite) and CC5 (42 wt% mica and 32 wt% illite/smectite) are respectively below or near the reactivity threshold at 7 and 14 days, suggesting low pozzolanic reactivity. CC56 (39 wt% mica, 3 wt% kaolinite, and 9 wt% illite/smectite) and CC31 (36 wt% mica, 13 wt% kaolinite, and 16 wt% illite/smectite) showed the highest reactivity, respectively 468 J/g of SCM and 330 J/g of SCM after 14 days. CC29 (18 wt% mica, 13 wt% kaolinite, and 7 wt% illite/smectite) showed moderate reactivity despite the higher kaolinite content (~11.5 wt%).

These observations confirm that micaceous phases and mixed mineral clay types significantly influence chemical reactivity. Samples with over 45 wt% micaceous content in the bulk clay, such as CC5 and CC28, exhibited reduced reactivity. When present in combination with other clay minerals, their influence does not follow a direct or predictable trend. Nevertheless, their pozzolanic reactivity may develop more slowly and they can still contribute meaningfully to the overall reactivity.

3.8. Correlating SSA and mineralogical composition of the raw clays

Given that pozzolanic reactivity evaluation, particularly the R^3 isothermal calorimetry test, is not always practical or feasible in industrial practice, potential correlations between physical and mineralogical properties of the evaluated clays were investigated. This considering that mineralogy seems to be the best indicator of pozzolanic reactivity of the calcined clays evaluated.

Fig. 18 shows the specific surface area (SSA) results for each of the groups adopted in this study.

Group 1 clays, with higher kaolinite contents, exhibited the lowest and most consistent SSA values, while **Groups 2** and **3** showed broader ranges linked to higher total clay and carbonate contents. **Group 4**, dominated by micaceous minerals, displayed the greatest variability. The pozzolanic reactivity of clays is influenced not only by chemical or mineralogical composition and structural disorder, but also by SSA, which is significantly affected by thermal treatment [32,88,89].

To determine the relationship between SSA and mineralogical composition of the raw clays, a Pearson correlation analysis was conducted. This method evaluates the strength and direction of linear relationships between two continuous variables [90]. The correlation coefficients (r) were calculated between SSA and individual mineral fractions in the low–purity raw clays (i.e. kaolinite, mica, smectite, illite/smectite, quartz, feldspars, among others). In addition to individual minerals, the analysis included composite variables such as total clay content, total clay minus mica content, and carbonate content (including calcite, dolomite, Fe–dolomite/ankerite). The resulting correlation matrix is visualized as a heatmap in Fig. 19.

The analysis did not reveal strong correlations (>0.7); however, consistent trends were observed. Quartz ($r = -0.50$) and kaolinite ($r = -0.31$) showed moderate negative correlations with SSA, suggesting that higher contents of these minerals tend to reduce the specific surface area. In contrast, smectite ($r = 0.48$), micas ($r = 0.13$), and carbonates ($r = 0.17$) showed weak positive correlations with SSA. These trends suggest that no single mineral controls the SSA, although certain minerals may influence it more significantly than others. Specifically, kaolinite–rich samples tend to exhibit lower and more consistent SSA values, whereas samples with higher smectite contents show generally higher SSA, complying with previous studies on argillaceous materials [56]. Overall, these relationships reflect the combined effects of mineralogical and textural factors, rather than a direct dependency on individual clay minerals.

3.9. Correlating chemical and mineralogical composition

To determine the relationship between the chemical and mineralogical composition of the raw clays, a Pearson correlation analysis was conducted, as explained in Section 3.8. Correlation coefficients (r) were calculated between major oxide contents (Al_2O_3, SiO_2, CaO, Fe_2O_3, MgO,

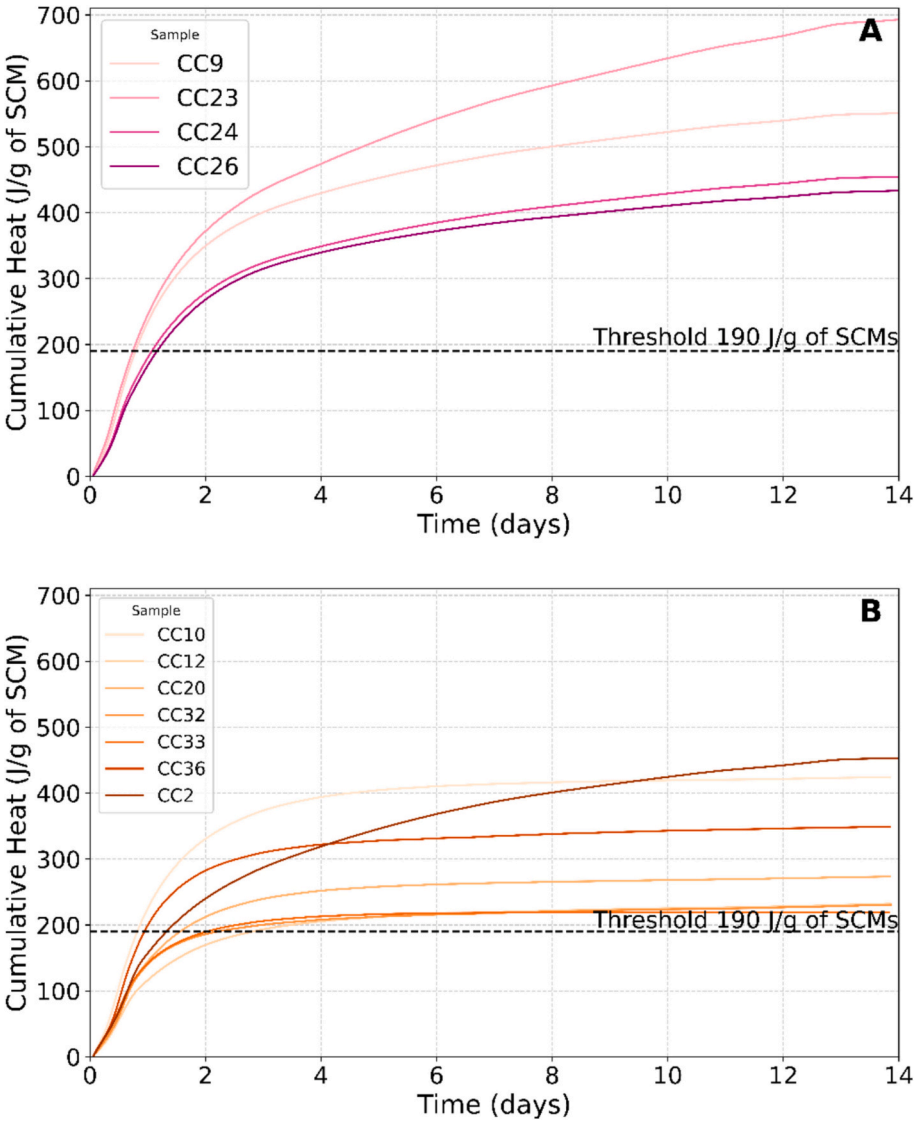

Fig. 17. R^3 cumulative heat curves of selected calcined clays from (A) Group 1, (B) Group 2, (C) Group 3 and (D) Group 4, up to 14 days of testing.

K_2O) and mineral fractions in the low–purity raw clays. Again, for this relationship, the analysis included composite variables such as total clay content, total clay minus mica content, and carbonate content, with the heatmap shown in Fig. 20.

The heatmap results revealed general trends of the relationship between chemical and mineralogical composition. With an *r* value of +0.7, the only strong positive correlation was between CaO content and carbonate levels, indicating that CaO increases directly with the carbonate content in the clays. Al_2O_3 showed a positive (but not very strong) correlation with kaolinite content ($r = +0.48$), with total clay content ($r = +0.35$), and with total clay content minus mica ($r = +0.39$). Apart from kaolinite, interlayered clays (illite/smectite) contribute to Al_2O_3 content ($r = +0.18$). A moderate positive correlation was also observed between MgO and chlorite ($r = +0.48$), as well as between MgO and K-feldspar ($r = +0.44$), confirming the association of Mg with chlorite (an Mg–bearing phyllosilicate), and it may also be linked to the presence of K-feldspar in specific lithologies (e.g. Lough Neagh Group, Gala Group). Similarly, K_2O correlated positively with chlorite ($r = +0.35$) and K–feldspar ($r = +0.43$), indicating that potassium is primarily associated with feldspathic phases and may also reflect contributions from partially weathered chlorite or illite.

The correlation analysis revealed that while certain oxides (e.g. Al_2O_3, Fe_2O_3, and SiO_2) may show moderate relationships with specific mineral phases, only CaO and carbonates exhibit a consistently strong linear relationship. This suggests that chemical composition alone does not provide a sufficiently robust or reliable proxy for quantitatively predicting clay mineral contents. The moderate correlations observed indicated that additional factors, such as complex mineralogy, crystallinity, particle size distribution, and the presence of mixed–layer phases, may also influence the chemical–mineralogical relationships in low–purity clays.

3.10. Correlating chemical reactivity with clay mineralogy

The R^3 cumulative heat evolution across the four groups of calcined clays revealed clear links between mineralogical composition and pozzolanic reactivity. R^3 isothermal calorimetry results for selected and grouped calcined clays are reported in Fig. 21, correlated with the mineralogical composition of the raw clays.

A reasonable positive correlation was observed between 14–day cumulative heat and kaolinite content (determined by QXRD) for Groups 1 and 2 (Fig. 21). Specifically, clays with kaolinite contents 20–40 wt%

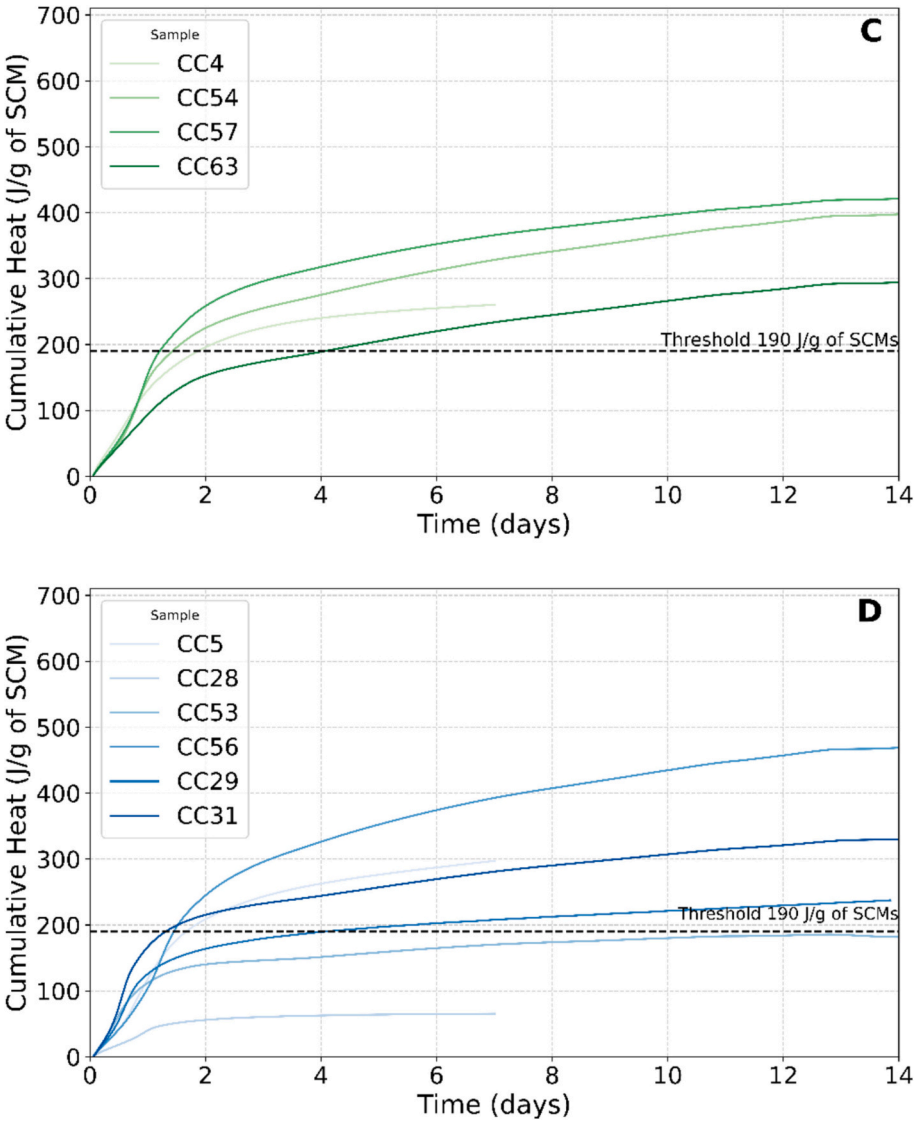

Fig. 17. (*continued*).

exhibited moderate reactivity (above the confidence value 190 J/g of SCMs [55]), while those with contents above 40 wt% typically achieved moderate to high reactivity (above 400 J/g of SCM [91]). This observation supports the use of kaolinite content as a useful, though not definitive, predictor of reactivity for certain clay groups (Group 1 in this study). However, this correlation does not hold for the carbonate–rich or micaceous clays, in Groups 3 and 4 respectively. These samples can exhibit moderate reactivity despite having high carbonates content or low kaolinite contents (<15 wt%), suggesting that other clay minerals or structural features contribute to reactivity.

Fig. 21B shows that total clay mineral content can serve as a broader indicator of chemical reactivity. While a loose clustering of higher reactivity values is observed within the 55–75 wt% total clay content range (green–shaded region), no strong or consistent correlation is apparent across all groups in this area. Group 1 and 2 samples with higher cumulative heat generally fall within this range. Despite mineralogical variability, all Group 3 samples exhibited moderate reactivity, indicating that such clays may still hold potential as SCMs. CC63 is considered an outlier in this analysis due to its composition (37.8 wt% calcite and 18 wt% dolomite) and is therefore classified as a calcareous clay. Although it achieved moderate reactivity, the sample does not follow the mineralogical thresholds proposed in this study. Group 4 samples displayed greater variability in performance, and their reactivity appears to be limited by their high mica content. Notably, sample CC28 emerges as an outlier in the correlation between total clay content and reactivity; although it contains approximately 60 wt% mica and 20 wt% mixed–layer mica/smectite, it exhibited negligible reactivity, reinforcing the limited contribution of micaceous minerals to pozzolanic performance upon thermal activation.

The variability in the R^3 14–day cumulative heat with small changes in mineralogy has practical relevance, demonstrating that low–purity clays with low kaolinite content could be suitable for use as SCMs in blended Portland cements [25], despite being considered unsuitable according to current guidelines for clay selection (e.g. kaolinite content) for SCMs production. These findings emphasise that while kaolinite content is a useful predictor for Groups 1 and 2, broader assessments of mineralogical composition are required to evaluate reactivity in more complex or lower–purity clays, which are shown to hold promising chemical reactivity potential.

To gain a more comprehensive understanding of the influence of mineralogical composition on the reactivity of low–purity clays, the fine fraction (< 2 μm) of selected samples was plotted on a ternary diagram (**Table S3** in the SI file). The corresponding 7 and 14–day cumulative heat release values were superimposed to illustrate compositional trends in reactivity (Fig. 22). Reactivity was represented through a categorical colour and shape coding scheme: unreactive (< 190 J/g SCM, red

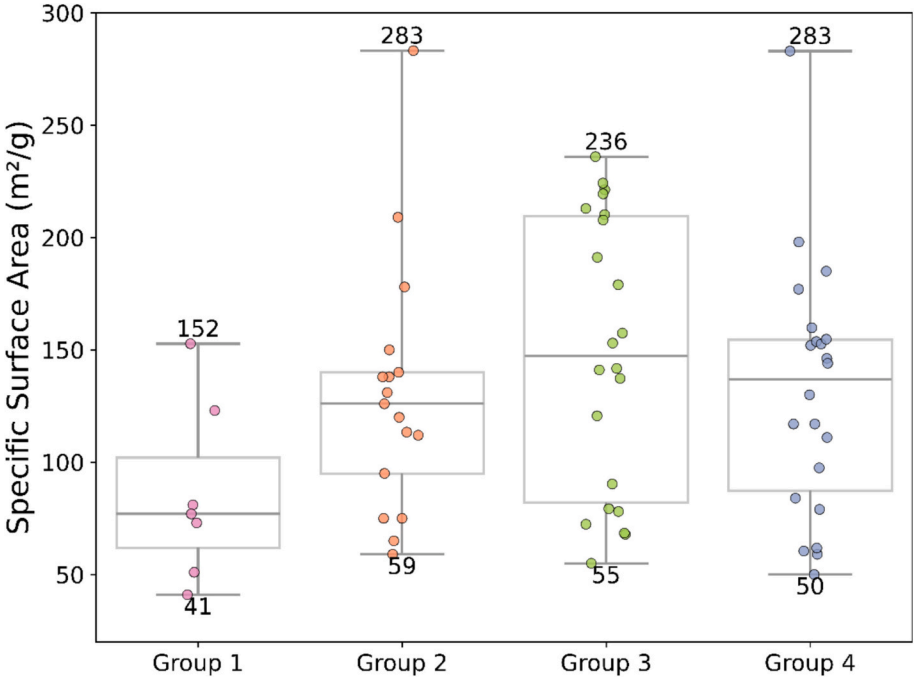

Fig. 18. Boxplot of specific surface area measurements for raw clay samples grouped by mineralogical criteria.

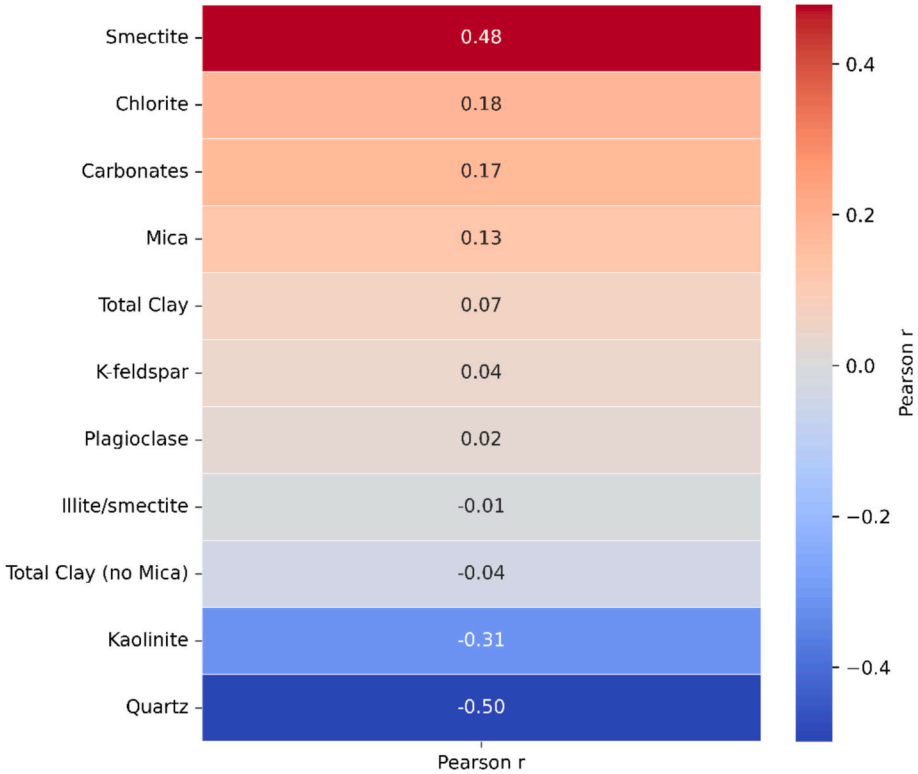

Fig. 19. Pearson correlation heatmap showing the relationship between SSA (x–axis) and selected mineralogical indicators (y–axis). Values range from −1 (strong negative correlation) to +1 (strong positive correlation), with colour gradients indicating the strength and direction.

symbols), moderately reactive (190–400 J/g SCM, blue), and highly reactive (> 400 J/g SCM, green). The ternary diagram is subdivided into reactivity fields to highlight the mineralogical domains associated with each reactivity class.

High reactivity is primarily associated with elevated kaolinite content in the fine fractions, often accompanied by moderate proportions of illite/smectite. These highly reactive samples cluster in the lower–right corner of the diagram, where kaolinite exceeds 40 wt%, mica is below 20 wt%, and illite/smectite ranges from 0 to 45 wt%, underscoring the dominant role of kaolinite in pozzolanic reactivity. The presence of disordered illite/smectite may further enhance reactivity through partial amorphization and dehydroxylation, whereas mica occurs only in

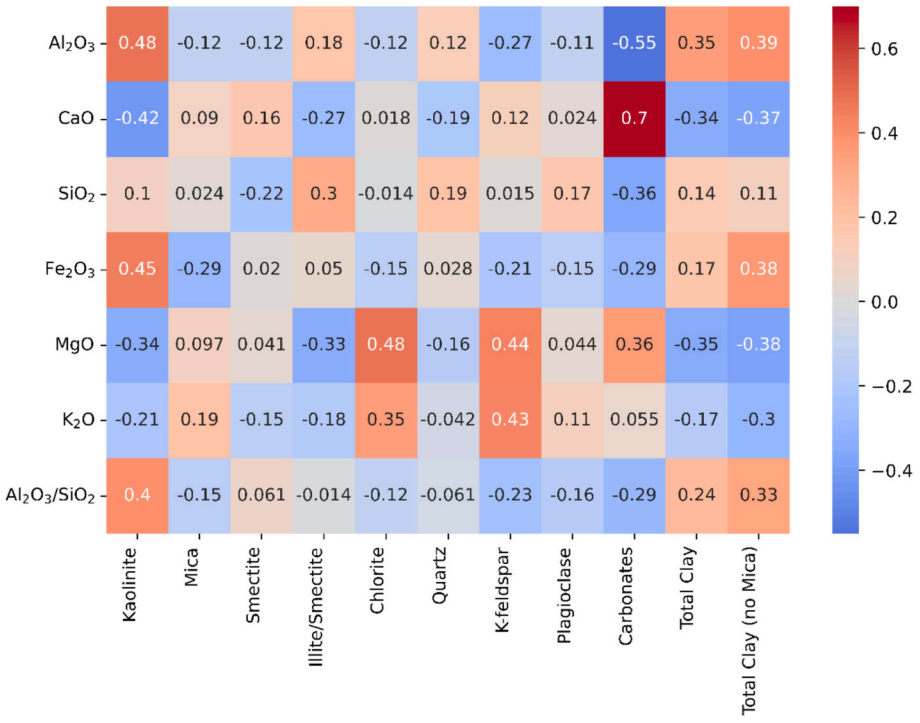

Fig. 20. Pearson correlation heatmap showing the relationship between selected oxides (y–axis) and selected mineralogical indicators (x–axis). Values range from −1 (strong negative correlation) to +1 (strong positive correlation), with colour gradients indicating the strength and direction.

minor amounts, consistent with its limited contribution to pozzolanic activity. Representative samples within this compositional domain include CC23, CC10, and CC9, all of which exhibited cumulative heat values exceeding 400 J/g SCM at 7 and 14 days.

Moderately reactive samples are more broadly distributed across the ternary diagram but tend to fall within a central domain characterised by balanced proportions of kaolinite and illite/smectite, with reduced mica contents. These compositions typically include 20–55 wt% kaolinite, 20–60 wt% mica, and 10–50 wt% illite/smectite. The reactivity of these clays also appears to benefit from the synergistic effect of moderate kaolinite content, and from the presence of disordered illite/smectite. Mica content remains moderate, limiting its inhibitory effect. These clays occupy a transitional compositional band between kaolinite– and mica–dominated fields. Representative samples within this category include C12, C33, C4, and C57, all of which exhibit cumulative heat release between 190 and 400 J/g SCM at 7 and 14 days.

In contrast, unreactive calcined clays are concentrated near the mica–rich corner of the ternary diagram, typically containing <20 wt% kaolinite and >60 wt% mica. This compositional range underscores the minimal contribution of micaceous phases to reactivity. Sample CC28 is part of this group, with negligible kaolinite content, over 60 wt% mica, and the lowest observed heat release.

In this study, all the selected calcined clays containing up to 24 wt% carbonates showed moderate reactivity. Mica content exceeding 60 wt% in the bulk fraction and 75 wt% in the clay fraction is considered a limiting factor for achieving sufficient pozzolanic reactivity. As per the illite/smectite content, the proportion should not exceed 60 wt% and should be balanced by a sufficient fraction of kaolinite (>30%) and limited mica content. The presence of quartz and feldspar in the bulk composition can influence the proportion of clay minerals and, therefore, the quantity of reactive phases available in the calcined clay. However, the results indicate that the mineralogical composition and distribution of the fine clay fraction (<2 μm) also play an important role in controlling chemical reactivity.

4. Influence of stratigraphy

For common clays, whilst the complexity and diversity of their mineralogy is well known, the full causal links between stratigraphy, mineralogical characteristics, and performance as an SCM are not yet well established. Previous studies [25,26] have largely focused on the links between the mineralogy of low-purity and common clays and pozzolanic reactivity determination. Extending this understanding across broader stratigraphic and geographic ranges has typically faced two main shortcomings: (i) detailed studies have investigated clays sourced from a single geological formation but have not compared clays between different formations; (ii) the source location or stratigraphy of sourced clays is not reported due to a lack of supplier information or commercial sensitivity. The availability of quality geological mapping data for the clays evaluated here makes it possible to further develop a geological connection with SCM selection.

In this study, five geological units were identified as containing clays with high potential as SCMs: the Etruria Formation, Pennine Middle and Lower Coal Measures formations, Avon Group, and Devensian Till (Table 4). Four of the formations examined are Carboniferous in age, ranging from early to late Carboniferous (Avon Group > Pennine formations > Etruria Formation). Despite their stratigraphic differences, they share a similar continental to paralic depositional environment, including floodplains, deltas, and coastal swamps – settings which favour the accumulation of fine–grained, clay–rich sediments. On the other hand, the Devensian Till is a Quaternary glacial deposit comprising a heterogeneous mixture of clay, deposited during the last glacial period. Although geologically young and compositionally variable, certain clay–rich tills may exhibit significant pozzolanic reactivity upon calcination, particularly when not extensively diluted by carbonates or sand and where favourable mineralogical assemblages are present.

Among the clays exhibiting moderate pozzolanic reactivity, their provenance includes nine distinct geological formations, as summarised in Table 4. These include several Carboniferous units with higher proportions of non–clay minerals, as well as formations from the Jurassic

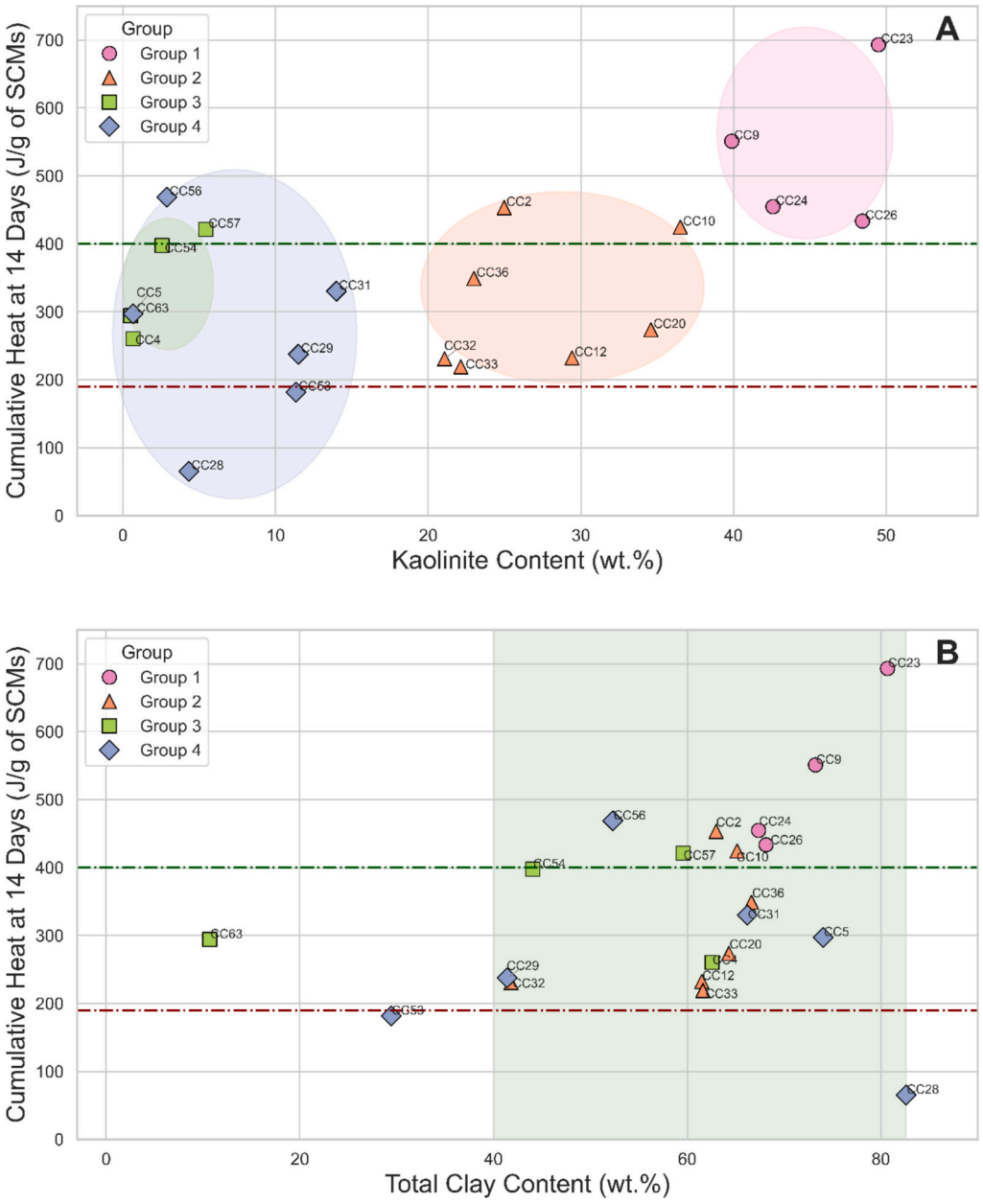

Fig. 21. Correlation between **(A)** the kaolinite content in the raw clays and their cumulative heat at 14 days according to the R^3–calorimetry method; and **(B)** the total clay content of the raw clays and their cumulative heat at 14 days according to the R^3–calorimetry method. The light green shaded region highlights the range of total clay contents (40–80 wt%) associated with SCMs that exhibit moderate to high pozzolanic reactivity. (For interpretation of the references to colour in this figure legend, the reader is referred to the web version of this article.)

(ranging from Early to Late), Quaternary, Early Cretaceous, and Late Triassic. Despite their varied geological ages, these formations share a common trait: they were deposited in low–energy environments such as delta plains (e.g., Millstone Grit, Coal Measures), floodplains (e.g., Alluvium/Glaciolacustrine), lakes and lagoons (e.g., Wealden Clay, Westbury Formation), and shallow marine shelves or basins (e.g., Ampthill, Rutland, Scunthorpe formations). These settings favoured the accumulation of fine–grained sediments but also led to the inclusion of interbedded siltstones, sands, ironstones, and limestones, resulting in heterogeneous mineralogical compositions. As a result, while these clays often lack the mineralogical purity of high reactivity kaolinitic formations such as the Etruria Formation or Coal Measures fireclays, they still offer moderate pozzolanic potential, particularly when appropriately processed or blended.

Fig. 23 shows the distribution of all collected samples according to their lithostratigraphy, classified by the mineralogically based grouping proposed in this study. Group 1 (red), representing high reactivity clays, is primarily concentrated in the Midlands and Pennine Basin, and corresponds to Carboniferous formations such as the Etruria Formation and Coal Measures, which are rich in fireclays and kaolinitic mudstones. Group 2 (orange), comprising moderately reactive clays, displays a broader geographical distribution across southern and eastern England (notably Jurassic and Cretaceous formations) as well as parts of Northern Ireland. Group 3 (green), characterised by carbonate-rich clays with moderate reactivity, is concentrated in central and southern England, reflecting the presence of Jurassic marls and carbonate-rich marine mudstones such as the Oxford and Ampthill Clay formations. Group 4 (blue), which includes mixed clays with varied low to moderate reactivity, is mostly found in Northern Ireland and western Scotland, and is associated with Tertiary and Quaternary deposits. The resulting map

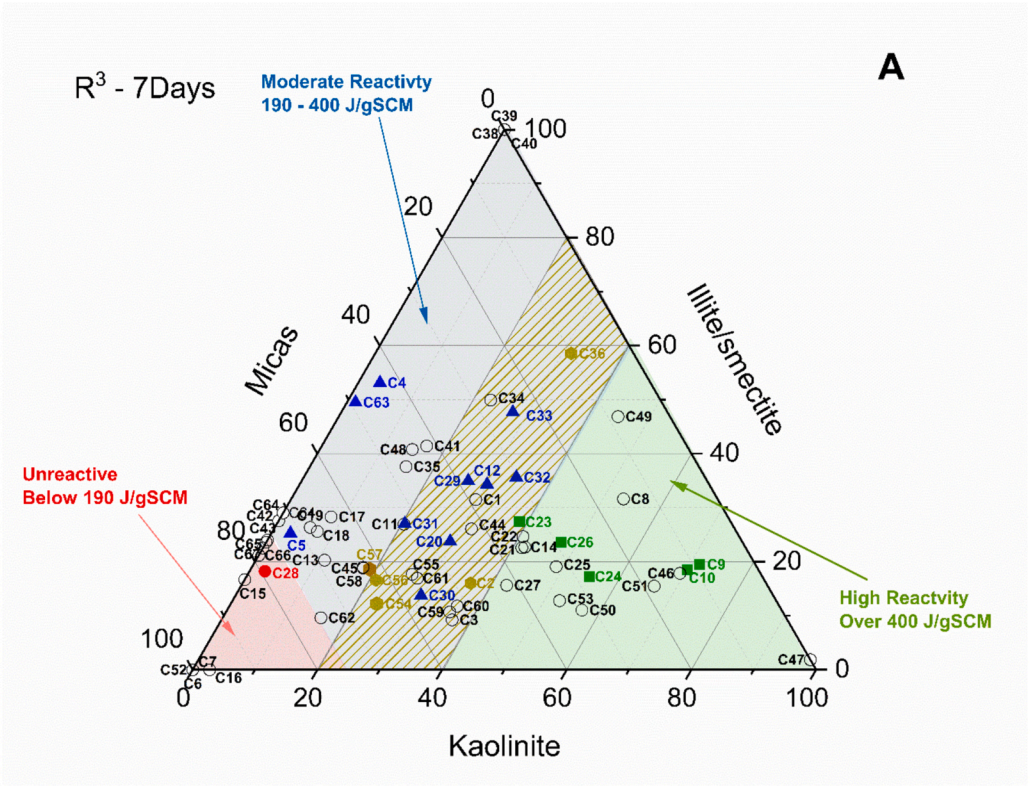

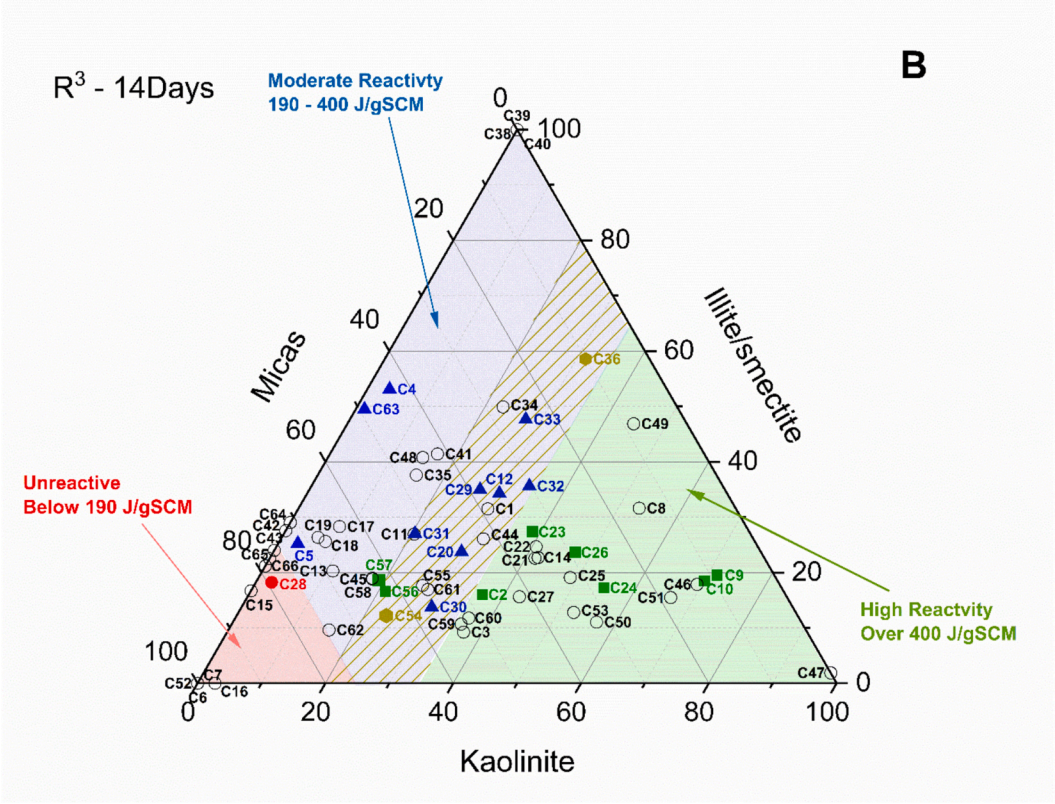

Fig. 22. Ternary diagrams showing the clay fraction (<2 μm) mineralogical composition of raw clays in terms of kaolinite, micas, and mixed–layer clays (smectite/illite), and their corresponding (A) 7 and (B) 14–day R^3 cumulative heat release, respectively. Reactivity thresholds and areas are indicated by symbol colour and shape: unreactive (<190 J/g SCM, red), moderately reactive (190–400 J/g SCM, blue), and highly reactive (>400 J/g SCM, green). (For interpretation of the references to colour in this figure legend, the reader is referred to the web version of this article.)

Table 4
Summary of the clay formations and their potential reactivity.

Stratigraphic classification	Reactivity classification
Etruria Formation;	
Pennine Middle Coal Measures Formation;	Over 400 J/g of SCMs
Avon Group;	High reactivity, high
Pennine Lower Middle Coal Measures Formation;	potential
Devensian Till;	
Millstone Grit Group;	
Pennine Middle Coal Measures Fm;	
Wealden Group;	
Wealden Clay Fm;	
Alluvium/ Glaciolacustrine, Devensian;	190–400 J/g of SCMs
Ampthill Clay Fm, Jurassic;	Moderate reactivity
Rutland Formation, Great Oolite Group, Middle Jurassic;	
Scunthorpe Mudstone Fm, Lias Group;	
Westbury Fm, Penarth Group, Triassic	

offers a valuable geospatial framework for identifying clay-rich geological units across the UK with potential for use in low–carbon cementitious applications. By linking geological formations to reactivity categories, it supports regionally informed SCM sourcing strategies, highlighting areas with the most promising raw materials for sustainable cement production.

5. Conclusions, implications and future research needs

This study provides a first–of–its–kind analysis of low–purity clays from the United Kingdom and a mineralogy-based framework for screening and comparing low-purity clay sources that can be used for producing suitable SCMs via calcination. Although the experimental dataset is UK-based, the analysis and results rely on fundamental mineralogical and lithological characteristics and are therefore transferable to clay resources in other regions exhibiting similar geological characteristics globally.

(a) Connecting mineralogical composition with chemical reactivity

Based on the mineralogical composition of the assessed low–purity clays, a classification system was developed, and the physical and chemical characteristics of the raw low–purity clays for each group are summarised in Table 5. In general, clays from Groups 1 and 2 present high to moderate chemical reactivity, when determined via R^3 testing, while clays from Group 3 and 4 present moderate to low reactivity. The chemical reactivity values are strongly dependent on the mineralogical features of each of the clay groups studied.

Reliance on 7-day cumulative heat from R^3 testing results can lead to disqualifying suitable clays that can be used as SCMs. It is recommended that the R^3 results of 7 days of testing (as per current standards) are evaluated in conjunction with R^3 testing results collected for at least 14 days, to enable selection of promising low-purity clay resources, accounting for their potentially ongoing pozzolanic reaction.

Based on the results, clays with a total clay mineral content of at least $\geq$40 wt%, and a mica content below 60 wt% in the clay mineral fraction were associated with moderate to high pozzolanic activity under the calcination conditions investigated. The presence of carbonates in low–purity clays should not be a criterion to disqualify a clay from SCM selection. This study demonstrates that carbonate–rich clays develop a moderate (for up to 30 wt% carbonates) to high (for up to 20 wt% carbonates) pozzolanic reactivity following calcination. However, further studies are needed to better define threshold values for carbonate contents in raw clay sources, and optimise processing conditions, to minimise the risk of reactive CaO formation. Moreover, calcination

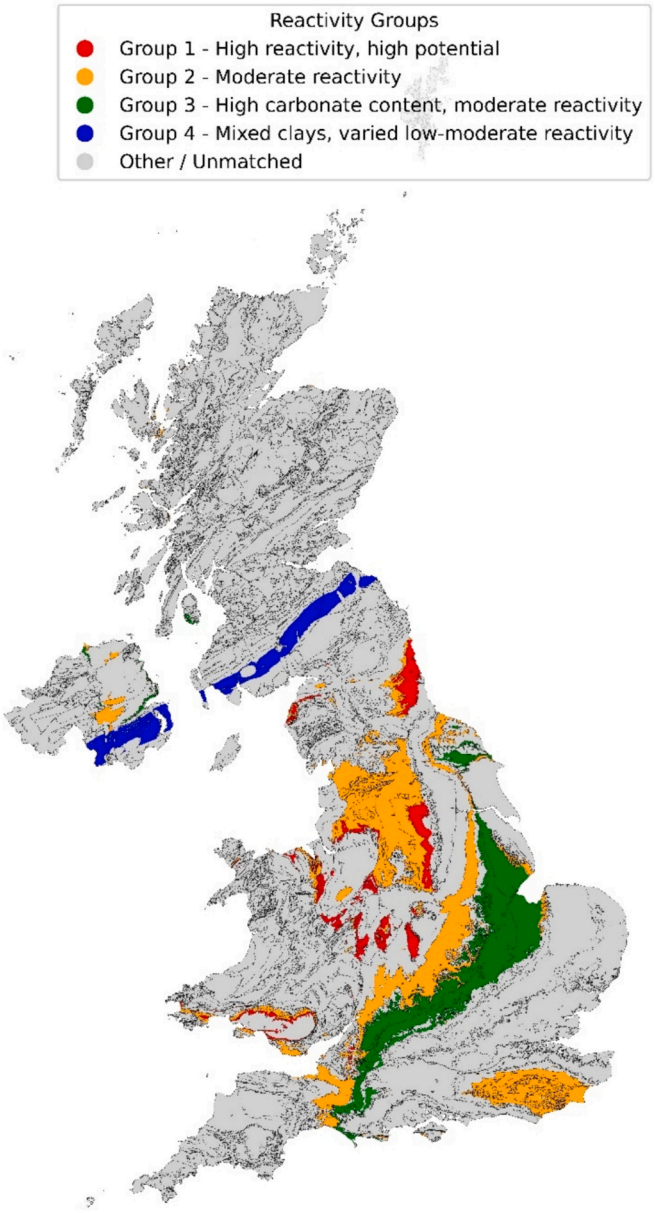

Fig. 23. Map of the United Kingdom showing the distribution of sampled geological formations, classified according to the mineralogically based reactivity groups defined in this study. Group 1 (red) represents high reactivity clays. Group 2 (orange) denotes clays of moderate reactivity. Group 3 (green) comprises carbonate rich clays, while Group 4 (blue) includes compositionally variable clays with generally low to moderate reactivity. Map generated with the data from BGS. (For interpretation of the references to colour in this figure legend, the reader is referred to the web version of this article.)

conditions of Group-3 clays can be further optimised, considering carbonates decomposition temperatures while inducing sufficient structural alterations in the clay minerals.

(b) Connecting chemical composition with chemical reactivity

A clear correlation between CaO and carbonate contents was identified, however, moderate correlations of other oxides with the bulk mineralogy of the raw clays suggest that chemical composition (e.g. Al_2O_3, SiO_2, among others) alone is an unreliable predictor of clay mineral content. Relying solely on chemical composition to select suitable clays may underestimate the pozzolanic potential of many

Table 5
Summary of the four classified clay groups based on key geochemical, mineralogical and physicochemical properties of the raw materials, including SiO_2 and Al_2O_3 content, kaolinite content, carbonate content, total clay content (all in wt%), specific surface area (SSA, m^2/g), and R^3 at 14 days.

Group number	Al_2O_3 content (wt%)	SiO_2 content (wt%)	Kaolinite content (wt%)	Carbonates content (wt%)	Total Clay content (wt%)	SSA (m^2/g)	R^3 at 14 days (J/g of SCM)
1	15–26	29–63	42–54	0	62–80	41–152	433–693
2	7–23	41–75	17–39	0–8	41–88	59–283	219–453
3	6–19	25–66	0–2	14–55	10–62	55–236	294–421
4	9–25	36–65	0–13	0–9	18–82	50–283	181–469

low–purity and common clays. Total clay mineral content is a more meaningful predictor of pozzolanic reactivity than oxide–based chemical thresholds alone. Moreover, total clay content is a better predictor of pozzolanicity than kaolinite content for low–purity clays with mixed clay mineralogy. Therefore, it is recommended that standards for activated clay-based SCMs move beyond purely chemical composition and kaolinite content-based thresholds and begin to incorporate mineralogical and performance-based criteria through reactivity testing, which more directly relate to pozzolanic reactivity.

(c) Connecting stratigraphy with reactivity

Links between the geological formation of clays, with their pozzolanic reactivity potential have been revealed. Low–purity clays derived from kaolinitic Carboniferous formations, such as the Etruria and Coal Measures, consistently exhibited moderate-to-high pozzolanic reactivity. Younger or marine–derived clays, particularly those from Jurassic, Cretaceous, and Quaternary units, tend to display more heterogeneous compositions with higher contents of mica, smectite, and carbonates, which limit their pozzolanic reactivity. Based on studies on a wide range of clay from different regions in the UK, Group 2 clays with 15–40% kaolinite and total clay mineral content >40% having a moderate reactivity are the widely available clay resource for calcined clay production.

(d) Implications and future research needs

This study demonstrates that existing criteria specified in guidelines and standards for qualifying potential clay resources as suitable SCMs are not effective for predicting the chemical reactivity of low-purity clays once calcined. Therefore, a step change in the rapid screening and selection of such resources is needed.

The guidelines developed here classify low-purity clays on their pozzolanic reactivity potential, based on their bulk mineralogical composition, establishing links between clay mineralogy and geological formations. Consequently, when using existing geological maps, it is possible to carried out regional-scale assessments of clay resources' suitability for calcined clay production. This new knowledge assists the exploration and sourcing of promising low-purity clays for SCMs production, in different geographical locations. It is worth noting that mineralogy characteristics are always determined and very well known in mining operations; therefore, the outcomes of this study have a significant practical importance.

However, further work is required to fully unlock the potential of low-purity clays as SCMs. The optimisation of the calcination parameters for clays with different mineralogy needs to be addressed, in order to maximise their reactivity. Moreover, SSA is an important parameter that indicates variations between clays, and its influence on pozzolanic reactivity was not fully addressed in this study. Future work should investigate the impact of SSA across different clays on their chemical reactivity once calcined.

The global geological diversity of clay deposits implies that additional datasets covering a broader range of clay types, impurity levels, mineralogy, and geology would strengthen the applicability of the proposed screening approach and refine the framework introduced here, supporting its implementation in industrial practice.

CRediT authorship contribution statement

Ilda Tole: Writing – review & editing, Writing – original draft, Methodology, Investigation, Formal analysis, Data curation, Conceptualization. **Yuvaraj Dhandapani:** Writing – review & editing, Investigation, Formal analysis, Data curation, Conceptualization. **Simon J. Kemp:** Writing – review & editing, Investigation, Formal analysis, Data curation. **Alastair T.M. Marsh:** Writing – review & editing, Conceptualization. **Clive Mitchell:** Writing – review & editing, Resources, Project administration, Funding acquisition. **Leon Black:** Writing – review & editing, Funding acquisition. **Hong Wong:** Writing – review & editing, Project administration, Funding acquisition. **Susan A. Bernal:** Writing – review & editing, Writing – original draft, Supervision, Project administration, Methodology, Funding acquisition, Formal analysis, Conceptualization.

Declaration of competing interest

The authors declare the following financial interests/personal relationships which may be considered as potential competing interests:

H. Wong, S.A. Bernal, C. Mitchell, S.J. Kemp, and L. Black report financial support was provided by the Engineering and Physical Sciences Research Council (EPSRC). I. Tole and Y. Dhandapani were supported by the research grants that sponsored this study, at the time the data was collected, and analysis was conducted.

S.A. Bernal serves as Editor of Cement and Concrete Research. She had no involvement in the peer review of this article and had no access to information regarding its peer review. Full responsibility for the editorial process for this article was delegated to another Editor. If there are other authors, they declare that they have no known competing financial interests or personal relationships that could have appeared to influence the work reported in this paper.

Acknowledgements

This study was sponsored by the UK Engineering and Physical Sciences Research Council (EPSRC) via the project 'Engineering UK clays for production of low–carbon cements'; through the awards EP/W021811/1, EP/W022583/1, EP/W021765/1. SJK and CJM publish with the permission of the Director of the BGS (UK Research and Innovation). Participation of S.A. Bernal in this study was also sponsored by EPSRC through the grant EP/R001642/1. The authors are grateful to the clay source owners for their valuable donation of samples, making this study possible. We also acknowledge the valuable discussions and comments from the industry partners and supporters of this project, which helped us to analyse the results considering practical needs for the widespread uptake of low–purity clays in industrial practice.

Appendix A. Supplementary data

Supplementary data to this article can be found online at https://doi.org/10.1016/j.cemconres.2026.108211.

Data availability

The database of this study is available in http://doi.org/10.5281/zenodo.18406772. For information about specific clay's locations please contact Dr. Clive Mitchel cjmi@bgs.ac.uk, and Dr. Simon Kemp sjk@bgs.ac.uk

References

[1] M.C.G. Juenger, R. Snellings, S.A. Bernal, Supplementary cementitious materials: new sources, characterization, and performance insights, Cem. Concr. Res. 122 (2019) 257–273, https://doi.org/10.1016/j.cemconres.2019.05.008.

[2] A.Z. Khalifa, Ö. Cizer, Y. Pontikes, A. Heath, P. Patureau, S.A. Bernal, A.T. M. Marsh, Advances in alkali–activation of clay minerals, Cem. Concr. Res. 132 (2020) 106050, https://doi.org/10.1016/j.cemconres.2020.106050.

[3] B. Lothenbach, K. Scrivener, R.D. Hooton, Supplementary cementitious materials, Cem. Concr. Res. 41 (2011) 1244–1256, https://doi.org/10.1016/j.cemconres.2010.12.001.

[4] Global Cement and Concrete Association (GCCA), Home page. https://gccassociation.org/, 2025.

[5] R.M. Andrew, Global CO_2 emissions from cement production, 1928–2018, Earth Syst. Sci. Data 11 (2019) 1675–1710, https://doi.org/10.5194/essd-11-1675-2019.

[6] Reclaimed calcined clay cements (Re-C3) report. https://cement.mineralproducts.org/Innovation/Reclaimed-calcined-clay-cements.aspx, 2025. (Accessed 21 April 2025).

[7] K.-C. Thienel, S. Scherb, N. Beuntner, M. Maier, R. Sposito, 1:1 or 2:1 – does it matter for calcined clay as supplementary cementitious material? Ce/Papers 6 (2023) 363–372, https://doi.org/10.1002/cepa.2775.

[8] R. Fernandez, F. Martirena, K.L. Scrivener, The origin of the pozzolanic activity of calcined clay minerals: a comparison between kaolinite, illite and montmorillonite, Cem. Concr. Res. 41 (2011) 113–122, https://doi.org/10.1016/j.cemconres.2010.09.013.

[9] S. Hollanders, R. Adriaens, J. Skibsted, Ö. Cizer, J. Elsen, Pozzolanic reactivity of pure calcined clays, Appl. Clay Sci. 132–133 (2016) 552–560, https://doi.org/10.1016/j.clay.2016.08.003.

[10] A.Z. Khalifa, Y. Pontikes, J. Elsen, Özlem Cizer, Comparing the reactivity of different natural clays under thermal and alkali activation, RILEM Tech Lett 4 (2019) 74–80. https://letters.rilem.net/index.php/rilem/article/view/85.

[11] M. Sharma, S. Bishnoi, F. Martirena, K. Scrivener, Limestone calcined clay cement and concrete: a state–of–the–art review, Cem. Concr. Res. 149 (2021) 106564, https://doi.org/10.1016/j.cemconres.2021.106564.

[12] S. Bishnoi, S. Maity, A. Mallik, S. Joseph, S. Krishnan, Pilot scale manufacture of limestone calcined clay cement: the Indian experience, Indian Concr. J 88 (6) (2014) 22–28.

[13] Y. Dhandapani, T. Sakthivel, M. Santhanam, R. Gettu, R.G. Pillai, Mechanical properties and durability performance of concretes with Limestone Calcined Clay Cement (LC3), Cem. Concr. Res. 107 (2018) 136–151, https://doi.org/10.1016/j.cemconres.2018.02.005.

[14] K. Scrivener, F. Avet, H. Maraghechi, F. Zunino, J. Ston, W. Hanpongpun, A. Favier, Impacting factors and properties of limestone calcined clay cements (LC3), Green Mater. 7 (2019) 3–14, https://doi.org/10.1680/jgrma.18.00029.

[15] D.D. Vallina, M.D. Rodríguez-Ruiz, I. Santacruz, A. Cuesta, M.A.G. Aranda, A.G. De la Torre, Supplementary cementitious material based on calcined montmorillonite standards, Constr. Build. Mater. 426 (2024) 136193, https://doi.org/10.1016/j.conbuildmat.2024.136193.

[16] N. Garg, J. Skibsted, Thermal activation of a pure montmorillonite clay and its reactivity in cementitious systems, J. Phys. Chem. C 118 (2014), https://doi.org/10.1021/jp502529d.

[17] C. He, E. Makovicky, B. Øsbæck, Thermal stability and pozzolanic activity of calcined illite, Appl. Clay Sci. 9 (5) (1995) 337–354, https://doi.org/10.1016/0169-1317(94)00033-M.

[18] E.F. Irassar, V.L. Bonavetti, C.C. Castellano, M.A. Trezza, V.F. Rahhal, G. Cordoba, R. Lemma, Calcined illite–chlorite shale as supplementary cementing material: thermal treatment, grinding, color and pozzolanic activity, Appl. Clay Sci. 179 (2019) 105143, https://doi.org/10.1016/j.clay.2019.105143.

[19] N.S. Msinjili, G.J.G. Gluth, P. Sturm, N. Vogler, H.-C. Kühne, Comparison of calcined illitic clays (brick clays) and low-grade kaolinitic clays as supplementary cementitious materials, Mater. Struct. 52 (2019) 94, https://doi.org/10.1617/s11527-019-1393-2.

[20] B. Ayati, D. Newport, H. Wong, C. Cheeseman, Low-carbon cements: potential for low-grade calcined clays to form supplementary cementitious materials, Cleaner Mater. 5 (2022) 100099, https://doi.org/10.1016/j.clema.2022.100099.

[21] S.S.E. Schulze, J. Rickert, Suitability of natural calcined clays as supplementary cementitious material, Cem. Concr. Compos. 95 (2019) 92–97, https://doi.org/10.1016/j.cemconcomp.2018.07.006.

[22] M. Maier, N. Beuntner, K.-C. Thienel, Mineralogical characterization and reactivity test of common clays suitable as supplementary cementitious material, Appl. Clay Sci. 202 (2021) 105990, https://doi.org/10.1016/j.clay.2021.105990.

[23] U. Mueller, G. Plusquellec, K. Malaga, Potential for use of activated clays in concrete in Sweden – roadmap, RISE Research Institutes of Sweden, Borås, 2021. Retrieved from https://urn.kb.se/resolve?urn=urn:nbn:se:ri:diva-57321.

[24] T. Danner, G. Norden, H. Justnes, Characterisation of calcined raw clays suitable as supplementary cementitious materials, Appl. Clay Sci. 162 (2018) 391–402, https://doi.org/10.1016/j.clay.2018.06.030.

[25] Y. Dhandapani, A.T.M. Marsh, S. Rahmon, F. Kanavaris, A. Papakosta, S.A. Bernal, Suitability of excavated London clay as a supplementary cementitious material: mineralogy and reactivity, Mater. Struct. 56 (2023) 174, https://doi.org/10.1617/s11527-023-02260-3.

[26] D. Zhou, R. Wang, M. Tyrer, H. Wong, C. Cheeseman, Sustainable infrastructure development through use of calcined excavated waste clay as a supplementary cementitious material, J. Clean. Prod. 168 (2017) 1180–1192, https://doi.org/10.1016/j.jclepro.2017.09.098.

[27] Y. Dhandapani, K.K. Subramanian, F. Kanavaris, L. Black, S.A. Bernal, The meta–kaolinite content of the calcined clay source impacts the mechanical and durability performance of blended Portland concrete, Cem. Concr. Res. 196 (2025) 107922, https://doi.org/10.1016/j.cemconres.2025.107922.

[28] R. Snellings, R. Almenares Reyes, T. Hanein, E.F. Irassar, F. Kanavaris, M. Maier, A. T. Marsh, L. Valentini, F. Zunino, A. Alujas Diaz, Paper of RILEM TC 282–CCL: mineralogical characterization methods for clay resources intended for use as supplementary cementitious material, Mater. Struct. 55 (2022) 149, https://doi.org/10.1617/s11527-022-01973-1.

[29] H.H. Murray, Chapter 8 common clays, in: H.H. Murray (Ed.), Dev, Clay Sci., Elsevier, 2006, pp. 141–145, https://doi.org/10.1016/S1572-4352(06)02008-3.

[30] T. Hanein, K.-C. Thienel, F. Zunino, A.T.M. Marsh, M. Maier, B. Wang, M. Canut, M.C.G. Juenger, M. Ben Haha, F. Avet, A. Parashar, L.A. Al-Jaberi, R.S. Almenares-Reyes, A. Alujas-Diaz, K.L. Scrivener, S.A. Bernal, J.L. Provis, T. Sui, S. Bishnoi, F. Martirena-Hernández, Clay calcination technology: state-of-the-art review by the RILEM TC 282-CCL, Mater. Struct. 55 (2021) 3, https://doi.org/10.1617/s11527-021-01807-6.

[31] C. He, E. Makovicky, B. Osbæck, Thermal stability and pozzolanic activity of raw and calcined mixed-layer mica/smectite, Appl. Clay Sci. 17 (2000) 141–161, https://doi.org/10.1016/S0169-1317(00)00011-9.

[32] A. Alujas, R. Fernández, R. Quintana, K.L. Scrivener, F. Martirena, Pozzolanic reactivity of low grade kaolinitic clays: influence of calcination temperature and impact of calcination products on OPC hydration, Appl. Clay Sci. 108 (2015) 94–101, https://doi.org/10.1016/j.clay.2015.01.028.

[33] S. Guggenheim, A.F. Koster van Groos, Baseline studies of the Clay Minerals Society source clays: thermal analysis, Clay Clay Miner. 49 (5) (2001) 433–443, https://doi.org/10.1346/CCMN.2001.0490509.

[34] C. He, B. Osbæck, E. Makovicky, Pozzolanic reactions of six principal clay minerals: activation, reactivity assessments and technological effects, Cem. Concr. Res. 25 (1995) 1691–1702, https://doi.org/10.1016/0008-8846(95)00165-4.

[35] A. Derkowski, A. Kuligiewicz, Thermal analysis and thermal reactions of smectites: a review of methodology, mechanisms, and kinetics, Clay Clay Miner. 70 (2022) 946–972, https://doi.org/10.1007/s42860-023-00222-y.

[36] S.C. Taylor-Lange, E.L. Lamon, K.A. Riding, M.C.G. Juenger, Calcined kaolinite-bentonite clay blends as supplementary cementitious materials, Appl. Clay Sci. 108 (2015) 84–93, https://doi.org/10.1016/j.clay.2015.01.025.

[37] A.T.M. Marsh, A.P. Brown, H.M. Freeman, A. Neumann, B. Walkley, H. Pendlowski, S.A. Bernal, Mineralogical characteristics influence the structure and pozzolanic reactivity of thermally and mechano-chemically activated meta-kaolinites, J. Mater. Chem. A 12 (2024) 24260–24277, https://doi.org/10.1039/D4TA02545H.

[38] N. Blouch, K. Rashid, I. Zafar, M. Ltifi, M. Ju, Prioritization of low-grade kaolinite and mixed clays for performance evaluation of limestone calcined clay cement (LC3): multi-criteria assessment, Appl. Clay Sci. 243 (2023) 107080, https://doi.org/10.1016/j.clay.2023.107080.

[39] S. Chatterji, Mechanism of expansion of concrete due to the presence of dead-burnt CaO and MgO, Cem. Concr. Res. 25 (1995) 51–56, https://doi.org/10.1016/0008-8846(94)00111-B.

[40] T. Schmidt, A. Leemann, E. Gallucci, K. Scrivener, Physical and microstructural aspects of iron sulfide degradation in concrete, Cem. Concr. Res. 41 (2011) 263–269, https://doi.org/10.1016/j.cemconres.2010.11.011.

[41] F. Zunino, K. Scrivener, Oxidation of pyrite (FeS_2) and troilite (FeS) impurities in kaolinitic clays after calcination, Mater. Struct. 55 (2021) 9, https://doi.org/10.1617/s11527-021-01858-9.

[42] F. Kanavaris, M. Vieira, S. Bishnoi, Z. Zhao, W. Wilson, A. Tagnit Hamou, F. Avet, A. Castel, F. Zunino, T. Visalakshi, F. Martirena, S.A. Bernal, M.C.G. Juenger, K. Riding, Standardisation of low clinker cements containing calcined clay and limestone: a review by RILEM TC-282 CCL, Mater. Struct. 56 (2023) 169, https://doi.org/10.1617/s11527-023-02257-y.

[43] ASTM C618-23, Standard specification for coal ash and raw or calcined natural pozzolan for use in concrete, ASTM International, West Conshohocken, PA, USA, 2023. https://www.astm.org/c0618-23.html.

[44] BS EN 196-5:2011, Methods of testing cement – part 5: pozzolanicity test for pozzolanic cement, European Committee for Standardization (CEN), Brussels, Belgium, 2011. https://knowledge.bsigroup.com/products/methods-of-testing-cement-pozzolanicity-test-for-pozzolanic-cement/standard. (Accessed 6 February 2025).

[45] BS EN 196-2:2013, Methods of testing cement – part 2: chemical analysis of cement, European Committee for Standardization (CEN), Brussels, Belgium, 2013. https://knowledge.bsigroup.com/products/methods-of-testing-cement-chemical-analysis-of-cement/standard. (Accessed 2 July 2025).

[46] R. Snellings, D. Londoño-Zuluaga, K. Scrivener, Interlaboratory test program to determine the precision of the R3 test method (ASTM C1897-20) for measuring reactivity of supplementary cementitious materials, Adv. Civ. Eng. Mater. 11 (2022) 500–519, https://doi.org/10.1520/ACEM20220023.

[47] NF P18-513:2012, Addition for concrete – metakaolin – specifications and conformity criteria, AFNOR Éditions / Association Française de Normalisation, Paris, France. https://www.boutique.afnor.org/en-gb/standard/nf-p18513/addition-for-concrete-metakaolin-specifications-and-conformity-criteria/fa175740/39605, 2012. (Accessed 29 May 2025).
[49] D.L. Carter, M.D. Heilman, C.L. Gonzales, Ethylene glycol monoethyl ether for determining surface area of silicate minerals, Soil Sci. 100 (1965) 356–360, https://web.archive.org/web/20100307061358id_/http://eprints.nwisrl.ars.usda.gov/308/1/35.pdf.
[50] S.J. Kemp, D. Wagner, The mineralogy, geochemistry and surface area of mudrocks from the London Clay Formation of southern England (Internal Report IR/06/060), British Geological Survey, Nottingham, UK, 2006. Available at: https://nora.nerc.ac.uk/id/eprint/7232/. (Accessed 21 April 2025).
[51] S.J. Kemp, D. Wagner, M.N. Ingham, The mineralogy, surface area and geochemistry of samples from the Wealden Group of southern England, in: British Geological Survey Internal Report, IR/10/079, UK, Keyworth, 2012. Available at: https://nora.nerc.ac.uk/id/eprint/19698. (Accessed 21 April 2025).
[52] R. Sposito, M. Maier, N. Beuntner, K.-C. Thienel, Physical and mineralogical properties of calcined common clays as SCM and their impact on flow resistance and demand for superplasticizer, Cem. Concr. Res. 154 (2022) 106743, https://doi.org/10.1016/j.cemconres.2022.106743.
[53] ASTM C1897-20, Standard Test Methods for Measuring the Reactivity of Supplementary Cementitious Materials by Isothermal Calorimetry and Bound Water Measurements, ASTM International, West Conshohocken, PA, USA, 2020, https://doi.org/10.1520/C1897-20.
[54] BS EN 196-12: 2024, Methods of testing cement – reactivity of cement constituents – heat of hydration and bound water content methods, BSI, London, UK, 2024. Available at: https://bsol.bsigroup.com/Bibliographic/BibliographicInfoData/000000000030470587. (Accessed 20 October 2025).
[55] D. Londono-Zuluaga, A. Gholizadeh-Vayghan, F. Winnefeld, F. Avet, M. Ben Haha, S.A. Bernal, Ö. Cizer, M. Cyr, S. Dolenec, P. Durdzinski, J. Haufe, D. Hooton, S. Kamali-Bernard, X. Li, A.T.M. Marsh, M. Marroccoli, M. Mrak, Y. Muy, C. Patapy, M. Pedersen, S. Sabio, S. Schulze, R. Snellings, A. Telesca, A. Vollpracht, G. Ye, S. Zhang, K.L. Scrivener, Report of RILEM TC 267-TRM Phase 3: validation of the R^3 reactivity test across a wide range of materials, Mater. Struct. 55 (2022) 142, https://doi.org/10.1617/s11527-022-01947-3.
[56] X. Zhu, J. Cai, G. Song, J. Ji, Factors influencing the specific surface areas of argillaceous source rocks, Appl. Clay Sci. 109–110 (2015) 83–94, https://doi.org/10.1016/j.clay.2015.02.016.
[57] S. Ferreiro, M.M.C. Canut, J. Lund, D. Herfort, Influence of fineness of raw clay and calcination temperature on the performance of calcined clay–limestone blended cements, Appl. Clay Sci. 169 (2019) 81–90, https://doi.org/10.1016/j.clay.2018.12.021.
[58] M. Atasever, S.T. Erdoğan, Effects of clay type and component fineness on the hydration and properties of limestone calcined clay cement, Mater. Struct. 57 (2024) 183, https://doi.org/10.1617/s11527-024-02461-4.
[59] A. Koutsouradi, T.R. Muzenda, P.A. Jensen, W.R. Leal da Silva, A.J. Damø, F. Georget, T. Matschei, Impact of clay calcination method on the physicochemical properties of limestone calcined clay cement, Constr. Build. Mater. 473 (2025) 140939, https://doi.org/10.1016/j.conbuildmat.2025.140939.
[60] R.J. Flatt, N. Roussel, H. Bessaies-Bey, L. Caneda-Martínez, M. Palacios, F. Zunino, From physics to chemistry of fresh blended cements, Cem. Concr. Res. 172 (2023) 107243, https://doi.org/10.1016/j.cemconres.2023.107243.
[61] M. Claverie, F. Martin, J.P. Tardy, M. Cyr, P. De Parseval, O. Grauby, C. Le Roux, Structural and chemical changes in kaolinite caused by flash calcination: formation of spherical particles, Appl. Clay Sci. 114 (2015) 247–255, https://doi.org/10.1016/j.clay.2015.05.031.
[62] R. San Nicolas, M. Cyr, G. Escadeillas, Characteristics and applications of flash metakaolins, Appl. Clay Sci. 83–84 (2013) 253–262, https://doi.org/10.1016/j.clay.2013.08.036.
[63] A. Koutsouradi, W.R. Leal da Silva, A.J. Damø, P.A. Jensen, Experimental investigation and comparison of soak and flash calcined kaolinite and montmorillonite, Appl. Clay Sci. 265 (2025) 107649, https://doi.org/10.1016/j.clay.2024.107649.
[64] M.F. Brigatti, E. Galan, B.K.G. Theng, Chapter 2: structures and mineralogy of clay minerals, in: F. Bergaya, B.K.G. Theng, G. Lagaly (Eds.), Developments in Clay Science, Elsevier, 2006, pp. 19–86, https://doi.org/10.1016/S1572-4352(05)01002-0.
[65] R. Snellings, P. Suraneni, J. Skibsted, Future and emerging supplementary cementitious materials, Cem. Concr. Res. 171 (2023) 107199, https://doi.org/10.1016/j.cemconres.2023.107199.
[66] BS EN 197-1:2011, Cement – composition, specifications and conformity criteria for common cements, BSI Standards Publication, London. https://knowledge.bsigroup.com/products/cement-composition-specifications-and-conformity-criteria-for-common-cements, 2019. (Accessed 29 May 2025).
[67] BS 8615-1:2019, Specification for pozzolanic materials for use with Portland cement – natural pozzolana and natural calcined pozzolana, BSI Standards Publication, London. https://knowledge.bsigroup.com/products/specification-for-pozzolanic-materials-for-use-with-portland-cement-natural-pozzolana-and-natural-calcined-pozzolana, 2019. (Accessed 17 May 2025).
[68] BS 8615-2:2019 Specification for pozzolanic materials for use with Portland cement – part 2: high-reactivity natural calcined pozzolana, BSI Standards Publication, London, UK, 2019. doi:https://doi.org/10.3403/30374452U (accessed May 17 2025).
[69] F.P. Glasser, D. Damidot, M. Atkins, Phase development in cement in relation to the secondary ettringite problem, Adv. Cem. Res. 7 (1995) 57–68, https://doi.org/10.1680/adcr.1995.7.26.57.
[70] M. Yamashita, T. Harada, E. Sakai, K. Tsuchiya, Influence of sulfur trioxide in clinker on the hydration heat and physical properties of Portland cement, Constr. Build. Mater. 250 (2020) 118844, https://doi.org/10.1016/j.conbuildmat.2020.118844.
[71] F.G. Bell, Fundamentals of Engineering Geology, Elsevier, 2016.
[72] F. Avet, K. Scrivener, Investigation of the calcined kaolinite content on the hydration of limestone calcined clay cement (LC3), Cem. Concr. Res. 107 (2018) 124–135, https://doi.org/10.1016/j.cemconres.2018.02.016.
[73] M. Dondi, M. Raimondo, C. Zanelli, Clays and bodies for ceramic tiles: reappraisal and technological classification, Appl. Clay Sci. 96 (2014) 91–109, https://doi.org/10.1016/j.clay.2014.01.013.
[74] K. Scrivener, F. Martirena, S. Bishnoi, S. Maity, Calcined clay limestone cements (LC3), Cem. Concr. Res. 114 (2018) 49–56, https://doi.org/10.1016/j.cemconres.2017.08.017.
[75] C. Emmanuel, P.K. Haldar, S. Maity, S. Bishnoi, Second pilot production of limestone calcined clay cement in India: the experience, Indian Concr. J. 90 (2016) 57–63.
[76] R. Snellings, Ö. Cizer, L. Horckmans, P.T. Durdziński, P. Dierckx, P. Nielsen, K. Van Balen, L. Vandewalle, Properties and pozzolanic reactivity of flash calcined dredging sediments, Appl. Clay Sci. 129 (2016) 35–39, https://doi.org/10.1016/j.clay.2016.04.019.
[77] F. Zunino, E. Boehm-Courjault, K. Scrivener, The impact of calcite impurities in clays containing kaolinite on their reactivity in cement after calcination, Mater. Struct. 53 (2020) 44, https://doi.org/10.1617/s11527-020-01478-9.
[78] R.A. Rowland, Differential thermal analysis of clays and carbonates, Clay Clay Miner. 1 (1955) 151–163, https://doi.org/10.1346/ccmn.1952.0010118.
[79] A.F. Gualtieri, S. Ferrari, Kinetics of illite dehydroxylation, Phys. Chem. Miner. 33 (2006) 490–501, https://doi.org/10.1007/s00269-006-0092-z.
[80] S.A. Bernal, M.C.G. Juenger, X. Ke, W. Matthes, B. Lothenbach, N. De Belie, J. L. Provis, Characterization of supplementary cementitious materials by thermal analysis, Mater. Struct. 50 (2016) 26, https://doi.org/10.1617/s11527-016-0909-2.
[81] M. Földvári, Handbook of Thermogravimetric System of Minerals and Its Use in Geological Practice, Geological Institute of Hungary, Budapest, 2011.
[82] K.S. Meyers, R.F. Speyer, Chapter 6 – thermal analysis of clays, in: M.E. Brown, P. K. Gallagher (Eds.), Handbook of Thermal Analysis and Calorimetry, Elsevier Science B.V, 2003, pp. 261–306, https://doi.org/10.1016/S1573-4374(03)80010-9.
[83] S.J. Kemp, A.L. Lewis, J.C. Rushton, Detection and quantification of low levels of carbonate mineral species using thermogravimetric–mass spectrometry to validate CO_2 drawdown via enhanced rock weathering, Appl. Geochem. 146 (2022) 105465, https://doi.org/10.1016/j.apgeochem.2022.105465.
[84] F. Avet, R. Snellings, A. Alujas Diaz, M. Ben Haha, K. Scrivener, Development of a new rapid, relevant and reliable (R3) test method to evaluate the pozzolanic reactivity of calcined kaolinitic clays, Cem. Concr. Res. 85 (2016) 1–11, https://doi.org/10.1016/j.cemconres.2016.02.015.
[85] Bureau of Indian Standards, IS 18189: 2023: Portland calcined clay limestone cement-specification. http://archive.org/details/gov.in.is.18189.2023, 2023. (Accessed 26 October 2025).
[86] T. Danner, G. Norden, H. Justnes, Calcareous smectite clay as a pozzolanic alternative to kaolin, Eur. J. Environ. Civ. Eng. 25 (2021) 1647–1664, https://doi.org/10.1080/19648189.2019.1590741.
[87] F. Bullerjahn, M. Zajac, J. Pekarkova, D. Nied, Novel SCM produced by the co-calcination of aluminosilicates with dolomite, Cem. Concr. Res. 134 (2020) 106083, https://doi.org/10.1016/j.cemconres.2020.106083.
[88] M.K. Chatterjee, D. Lahiri, Pozzolanic activity in relation to specific surface of some artificial pozzolanas—part I: measurement of surface area from water adsorption isotherms, Trans. Indian Ceram. Soc. 26 (1967) 65–70, https://doi.org/10.1080/0371750X.1967.10855587.
[89] M.K. Chatterjee, D. Lahiri, Pozzolanic activity in relation to specific surface of some artificial pozzolanas—part II: relationship between pozzolanic activity and specific surface, Trans. Indian Ceram. Soc. 26 (1967) 71–74, https://doi.org/10.1080/0371750X.1967.10855588.
[90] Z. Li, X. Gao, D. Lu, Correlation analysis and statistical assessment of early hydration characteristics and compressive strength for multi-composite cement paste, Constr. Build. Mater. 310 (2021) 125260, https://doi.org/10.1016/j.conbuildmat.2021.125260.
[91] P. Suraneni, A. Hajibabaee, S. Ramanathan, Y. Wang, J. Weiss, New insights from reactivity testing of supplementary cementitious materials, Cem. Concr. Compos. 103 (2019) 331–338, https://doi.org/10.1016/j.cemconcomp.2019.05.017.